Calcium:

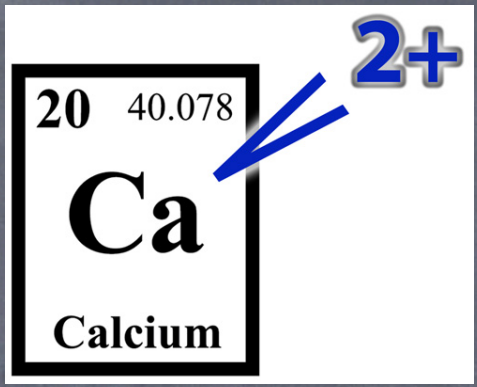

- is a universal intracellular messenger
- is involved in the regulation of virtually all cellular functions
- can be measured in living cells using specific fluorescent/luminescent probes

THE VERSATILITY AND UNIVERSALITY OF CALCIUM SIGNALLING

Michael J. Berridge, Peter Lipp and Martin D. Bootman

INNOVATION

Looking forward to seeing calcium

Rüdiger Rudolf, Marco Mongillo, Rosario Rizzuto and Tullio Pozzan

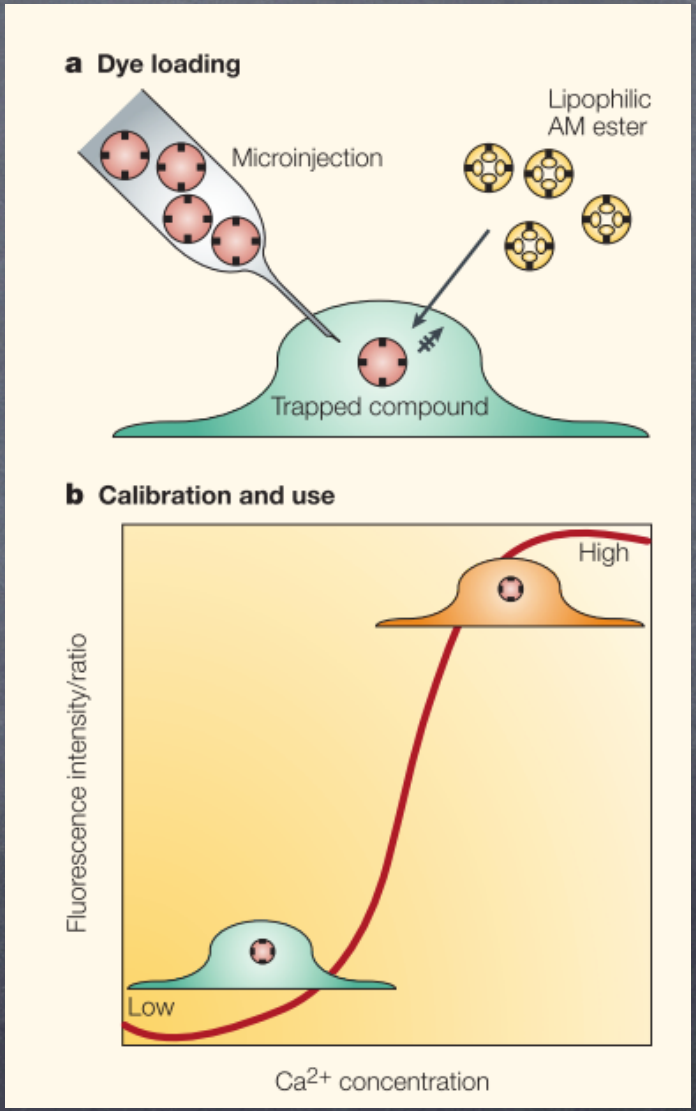

Box 1 | **Ca^{2+} sensors**

Ratiometric dyes

The excitation (or emission) spectrum (see figure, part **a**) of ratiometric dyes, such as fura-2 and indo-1, changes according to the free Ca^{2+} concentration, $[Ca^{2+}]$. The Ca^{2+} concentration is measured as the ratio between two fluorescence intensity values that are taken at two wavelengths, λ1 and λ2. Ratiometric dyes correct for unequal dye loading, bleaching and focal-plane shift, for example, as the ratio does not depend on the absolute intensity of the two signals. This can be illustrated by a simple example: if there are two cells, A and B, that have the same intracellular Ca^{2+} concentration, $[Ca^{2+}]_i$, but different concentrations of the dye, the ratio between the two wavelengths will immediately reveal that their $[Ca^{2+}]_i$ is identical, whereas a complex calibration procedure would be necessary to obtain the same information with an indicator that only changes its intensity as a function of Ca^{2+} concentration.

Non-ratiometric dyes

Ca^{2+} concentration is determined solely by a relative increase in the fluorescence intensity (see figure, part **b**) of non-ratiometric dyes, such as fluo dyes and rhod dyes, on elevation of the free Ca^{2+} concentration. The single excitation allows for simpler instrumentation or simultaneous observation of other parameters. These dyes mainly work in the visible range.

It should be noted that dyes are available with a range of K_d values and spectral properties that make them suitable for use at common laser lines, and some of the single-wavelength indicators give extremely strong fluorescence changes on Ca^{2+} binding. It is also important to note that relative, approximate, and not absolute, Ca^{2+} concentration values are usually all that is measured. Measuring the Fmin/Fmax or Rmin/Rmax values in cells or tissues requires the exposure of the dye within intact cells to a known Ca^{2+} concentration by harsh biochemical methods, such as high doses of ionophores, that are often incompatible with cell survival. This is an even bigger problem with probes targeted to organelles. AU, arbitrary units; F, fluorescence intensity; Fmax, F at saturating Ca^{2+} concentration; Fmin, F at zero Ca^{2+} concentration; K_d, dissociation constant; R, ratio between two wavelengths; Rmax, R at saturating Ca^{2+} concentration; Rmin, R at zero Ca^{2+} concentration; Sb2, value at saturating Ca^{2+} concentration for wavelength two; Sf2, value at zero Ca^{2+} concentration for wavelength two.

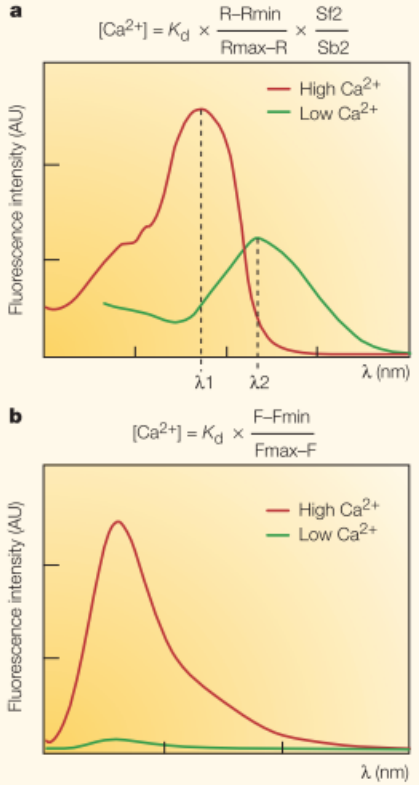

Box 2 | **Protein-based Ca^{2+} sensors**

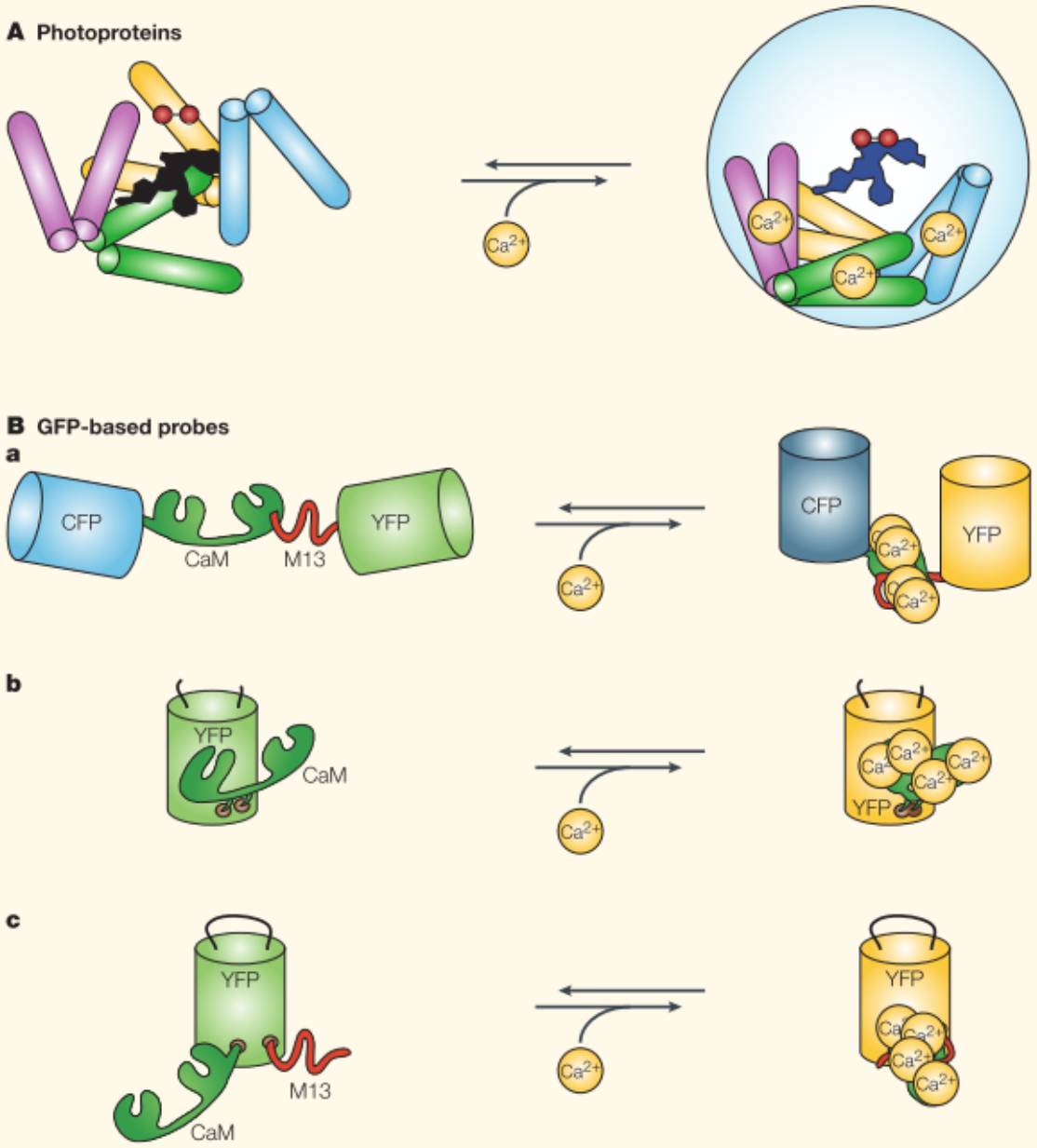

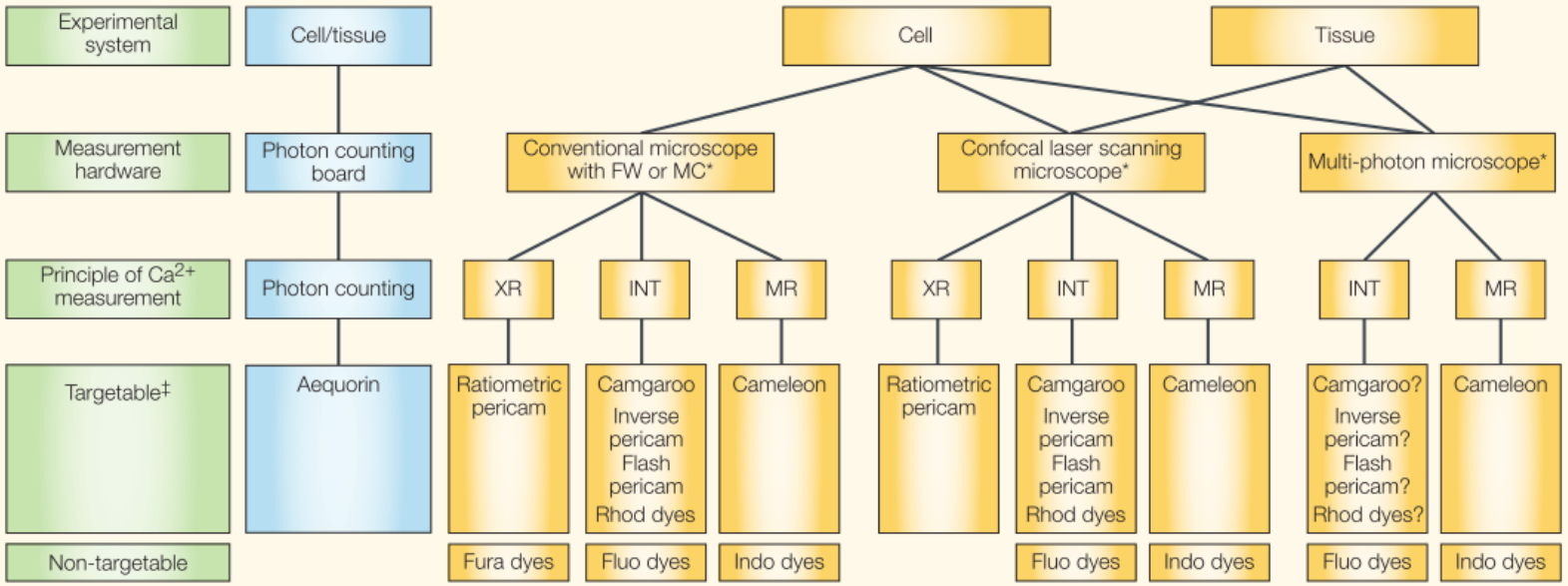

Figure 4 | **Description of major decisions for the planning of a Ca^{2+}-concentration imaging experiment.** The flow chart summarizes the main decisions to be made in a typical Ca^{2+}-concentration imaging experiment (left column, green) and the corresponding hardware that is available at present for each of these steps (right columns, blue and yellow). At certain points, according to the experimental approach, there are several choices of hardware, which are indicated by forked lines. *The use of a monochromator increases the time resolution considerably when compared with filter wheel-equipped microscopes. While the costs associated with confocal laser scanning microscopy are considerably higher than those associated with conventional microscopy, the costs associated with multi-photon microscopy are even greater. ‡Note that targeted chemical probes are only available in the form of rhod2 for mitochondria. Low-affinity dyes could be used under certain instances for Ca^{2+}-concentration measurements in the endoplasmic reticulum. FW, filter wheel; INT, intensity measurement; MC, monochromator; MR, emission ratioing; XR, excitation ratioing.

Table 1 | **The 'ideal' Ca^{2+} probe and the status of indicators available at present**

Probe	Fluorescence	Spectral shift	Ca^{2+} specificity	Toxicity	Targetability	Variable Ca^{2+} affinity	pH sensitivity	Molecular mass
'Ideal' probe	Strong	Yes	High	None	Yes	Yes	None	Variable
Synthetic polycarboxylates	Variable*	Some yes, but only in the UV range	Good‡	In the short term, relatively low	Poor (except for Rhod-2)	Yes	Only below about pH 6.5	Variable§
GFP-based probe	Variable	Some yes, and in the visible range	Good	ND	Yes	Yes	Generally high	Limited variability (44–83 kDa)

*The new generation of polycarboxylates are quite variable in terms of the fluorescence intensities of the Ca^{2+}-free and Ca^{2+}-bound forms. Some are strongly fluorescent without Ca^{2+}, but the changes on Ca^{2+} binding are relatively small (for example, Oregon Green), whereas others are very dim without Ca^{2+} and the fluorescence increases many times on Ca^{2+} binding (for example, fluo-3). ‡Although the Ca^{2+} selectivity over Mg^{2+} and monovalent cations of most polycarboxylate indicators is very good, they bind with a significantly higher affinity than other divalent and trivalent cations. §Although the molecular mass of all polycarboxylate indicators is about 1 kDa, they can be conjugated to dextrans of different molecular weights. GFP, green fluorescent protein; ND, not determined; UV, ultraviolet.

Interaction with other intracellular pathways
(cAMP, InsP3, Nitric oxide, Arachidonic acid…)

Spatio-temporal restrictions
(compartmentalization, intracellular distribution and targeting, polarization…)

Physio-pathological effects
(fluid secretion, cardiac functions, development of the nervous system, neovascularization…)

Intracellular calcium homeostasis at resting conditions is highly compartimentalized and its concentration in the cytosol - [Ca]c - is maintained low (50-100 nM) by energy consumption

passive permation: ion channels

ON reactions: cytosolic calcium increases

active permeation:

antiporters (NCX)

pumps (PMCA and SERCA)

OFF reactions: cytosolic calcium decreases

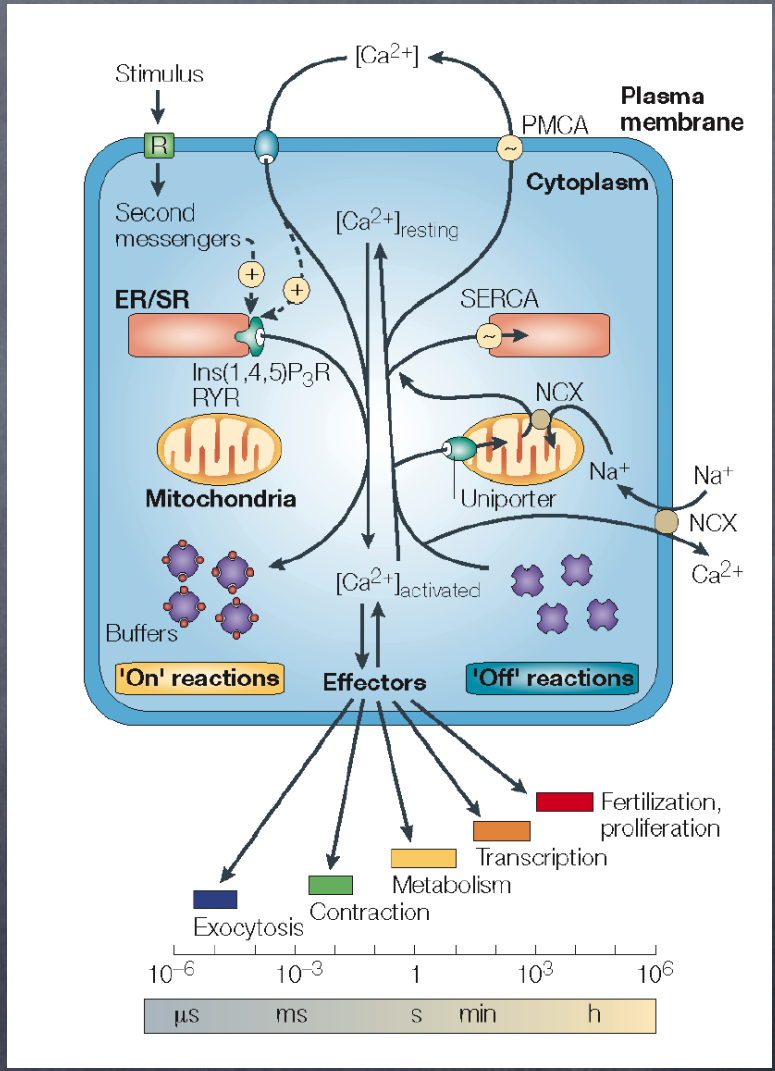

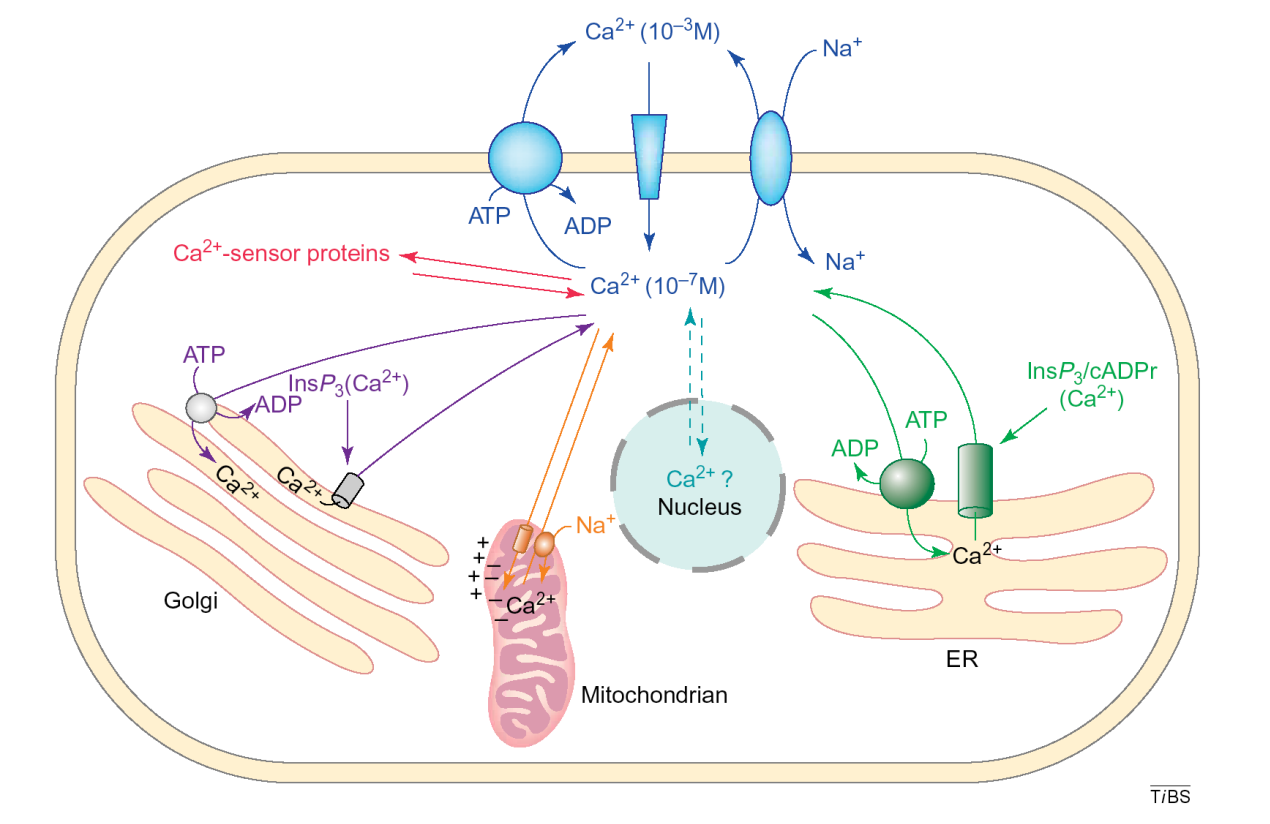
Ca2+ (10−3M)
Na+
ATP
ADP
Ca2+-sensor proteins
Ca2+ (10−7M)
Na+
ATP
InsP3(Ca2+)
ADP
Ca2+
Ca2+
Golgi
Na+
Ca2+
Mitochondrian
Ca2+ ?
Nucleus
InsP3/cADPr
(Ca2+)
ATP
ADP
Ca2+
ER
TiBS

CALCIUM SIGNALING
is the response to external stimula

Calcium signalling:

1. perceive — spatiotemporal pattern of calcium changes
2. transduce — calcium sensors
3. respond — calcium effectors and cell response

CALCIUM SIGNALING
is the response to external stimula

Calcium signalling:

1. perceive spatiotemporal pattern of calcium changes

2. transduce calcium sensors

3. respond calcium effectors and cell response

Calcium Signaling

Martin D. Bootman

The Babraham Institute Babraham Research Campus, Cambridge CB22 3AT, United Kingdom

Correspondence: martin.bootman@bbsrc.ac.uk

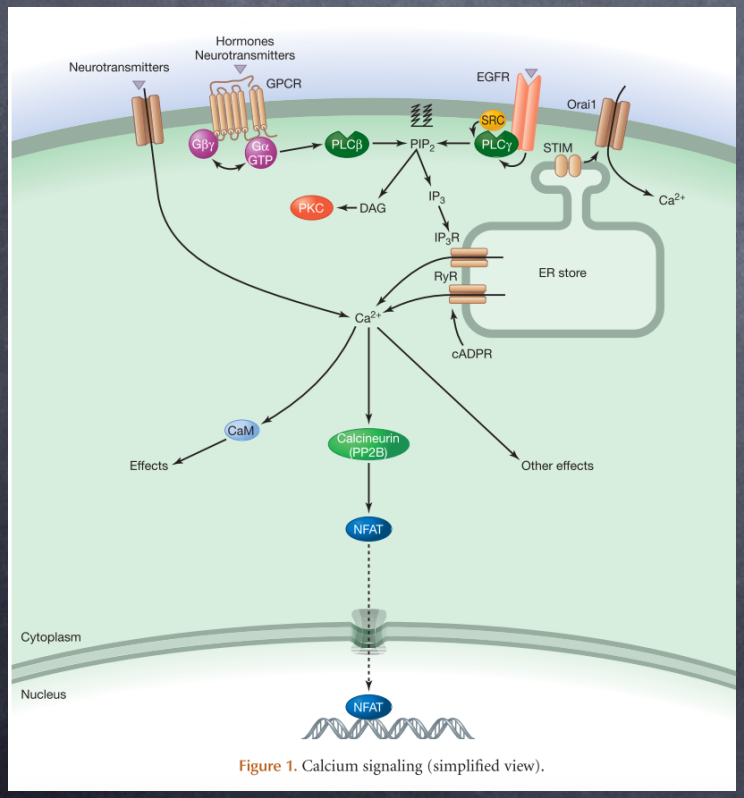

Figure 1. Calcium signaling (simplified view).

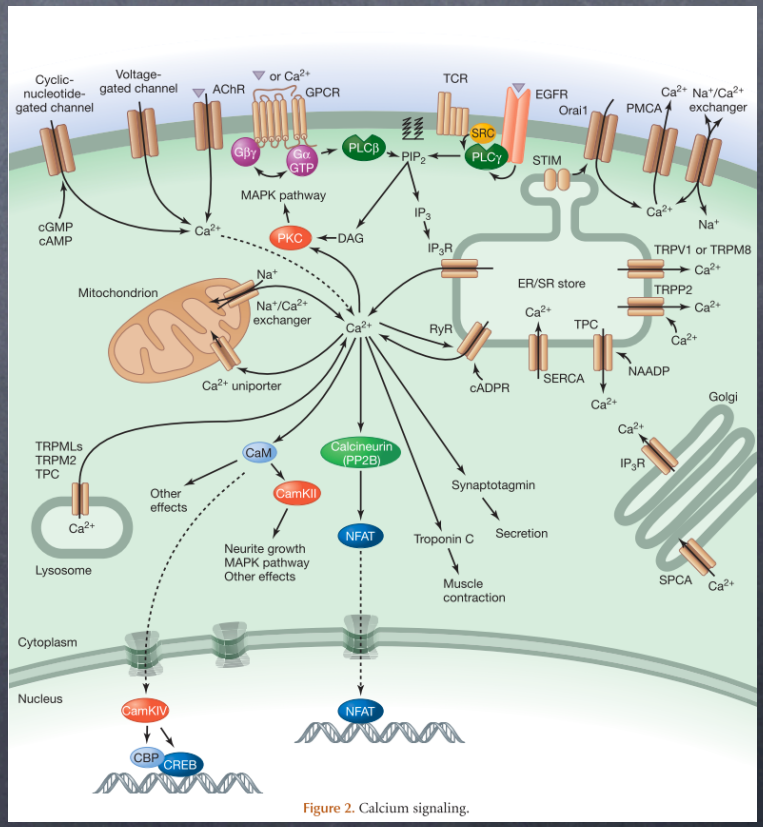

Figure 2. Calcium signaling.

1. **calcium signature** generated by an external stimulus (agonist): channels, pumps, transporters, buffers

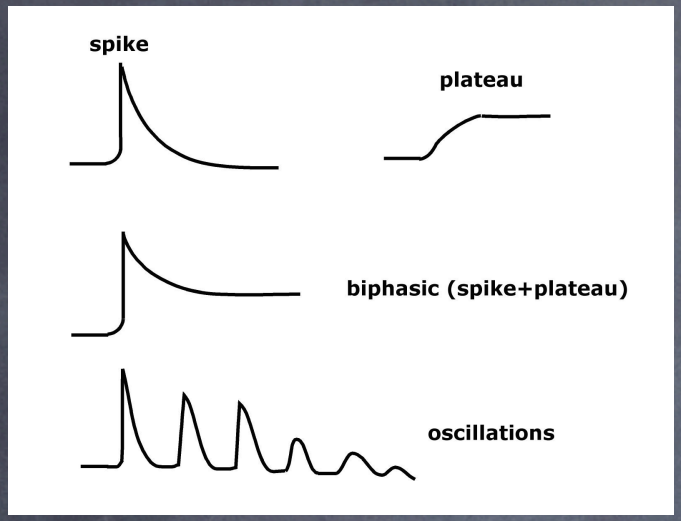

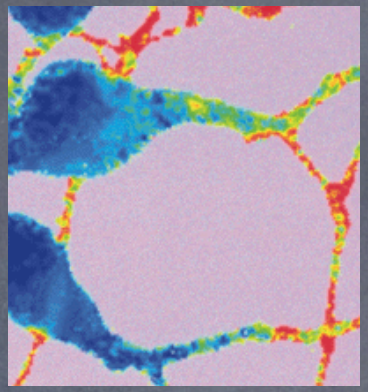

3 parameters: Amplitude

Time course

Spatial distribution

Extracellular agonists usually increase [Ca]c by activation of

1. calcium entry from extracellular medium

Voltage operated channels (Ca_v)

Voltage independent channels
- store operated calcium entry (SOCE)
- store independent calcium entry (NSOCE)

2. calcium release from intracellular stores

mediated by intracellular messengers (InsP3…)

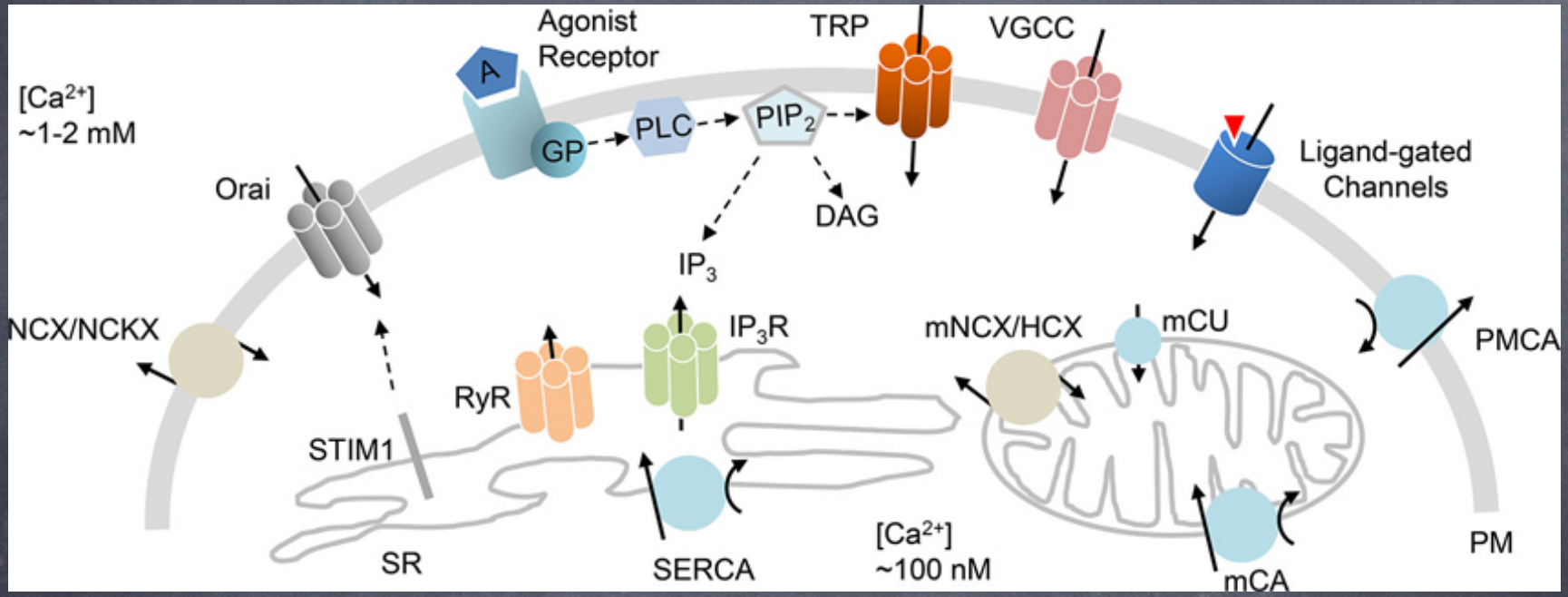
Agonist
Receptor
TRP
VGCC
[Ca2+]
~1-2 mM
A
GP
PLC
PIP2
Ligand-gated
Channels
Orai
DAG
IP3
NCX/NCKX
IP3R
mNCX/HCX
mCU
PMCA
RyR
STIM1
SR
SERCA
[Ca2+]
~100 nM
mCA
PM

Multiple regulations of calcium channels

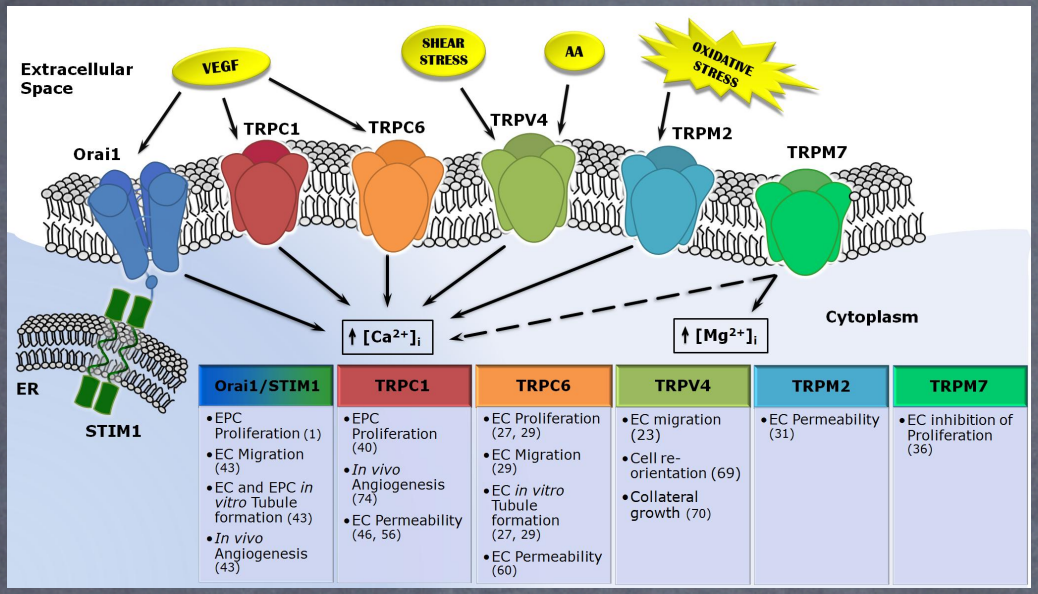

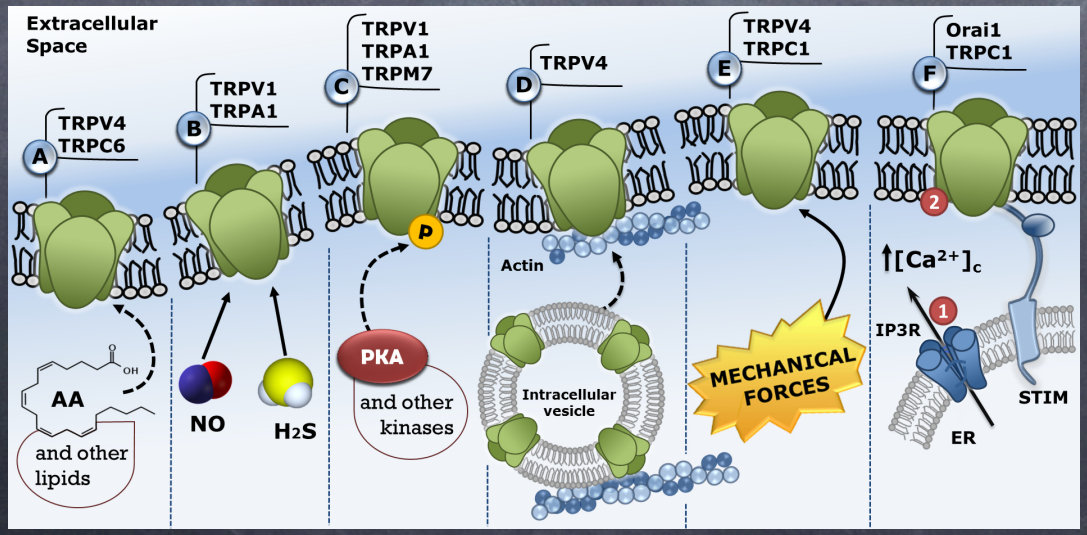

STORE-INDEPENDENT CALCIUM ENTRY (NSOCE)

STORE-DEPENDENT CALCIUM ENTRY (SOCE)

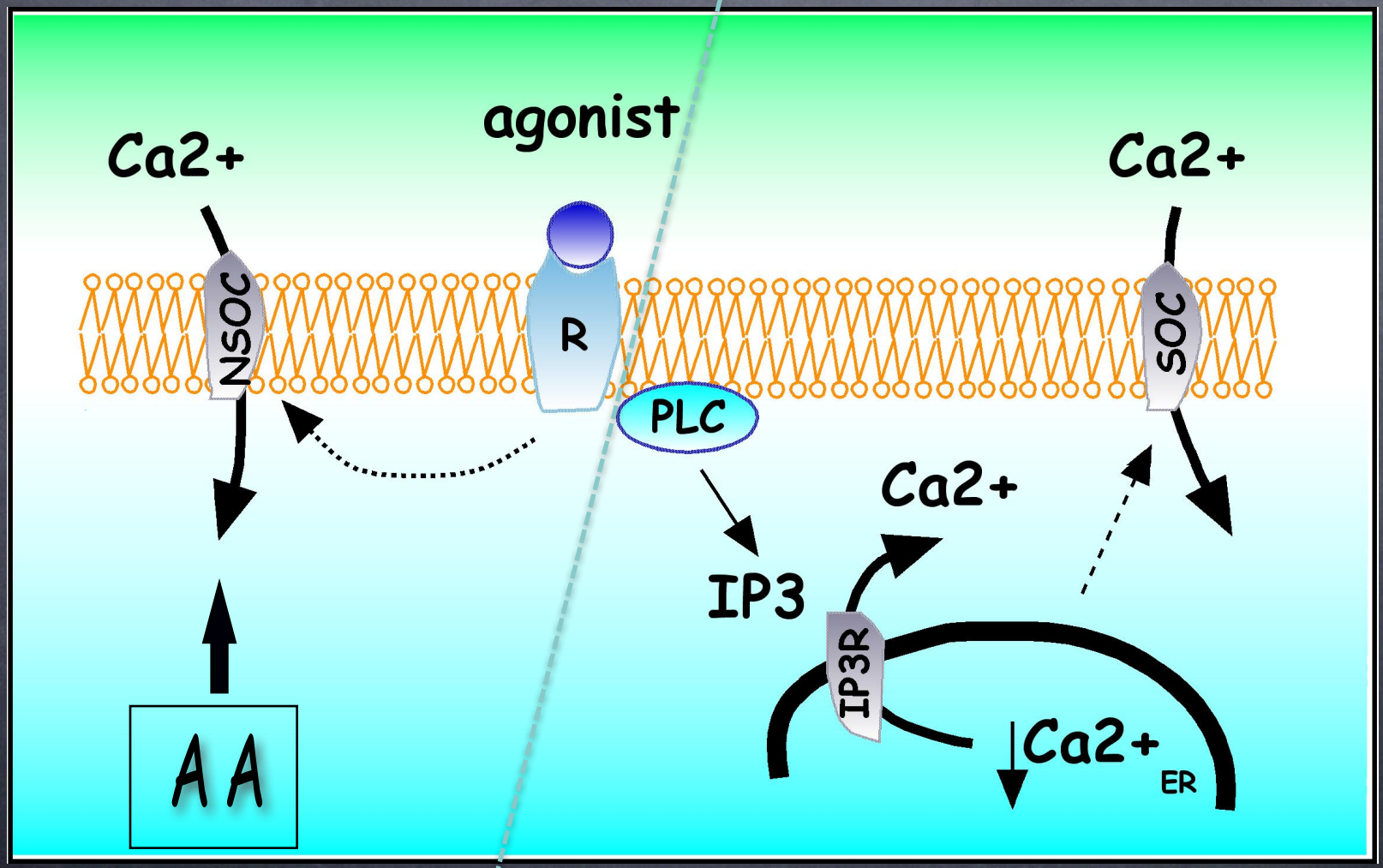

J Pharmacol Sci **125**, 340 – 346 (2014)

Journal of Pharmacological Sciences

Current Perspective

Key Components of Store-Operated Ca^{2+} Entry in Non-Excitable Cells

Yosuke Tojyo[1,2,*], Takao Morita[1], Akihiro Nezu[1], and Akihiko Tanimura[1]

[1]*Department of Pharmacology,* [2]*Laboratory of Biophysics, School of Dentistry, Health Sciences University of Hokkaido, Ishikari-Tobetsu, Hokkaido 061-0293, Japan*

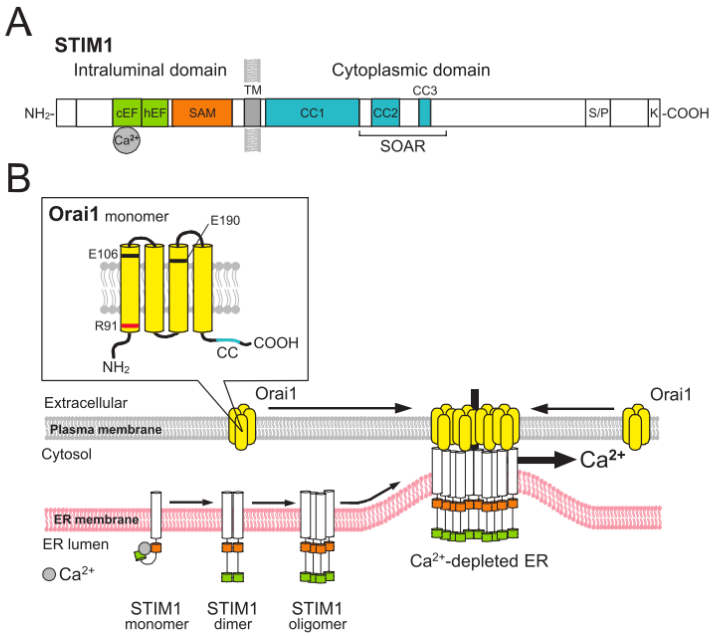

Fig. 1. Current model of store-operated Ca^{2+} entry. A) Domain structure of STIM1. The N-terminus of STIM1 includes a canonical Ca^{2+}-binding EF-hand (cEF), a hidden EF-hand (hEF), and a sterile α motif (SAM), followed by the transmembrane domain (TM). The SAM domain contributes to STIM1 oligomerization. The C-terminus includes three coiled-coil domains (CC1-3), a serine/proline-rich domain (S/P), and a lysine-rich domain (K). CC2 and CC3 are part of the STIM-Orai activating region (SOAR), which is involved in the activation of Orai channels (24). B) Coupling between STIM1 and Orai1. Depletion of Ca^{2+} in the ER causes Ca^{2+} dissociation from the STIM1 N-terminal cEF-hand, resulting in STIM1 oligomerization and translocation to ER-PM junctions. There, the STIM1 oligomers interact with diffusible Orai1 tetramers in the PM and activate Orai1 channels, leading to Ca^{2+} entry.

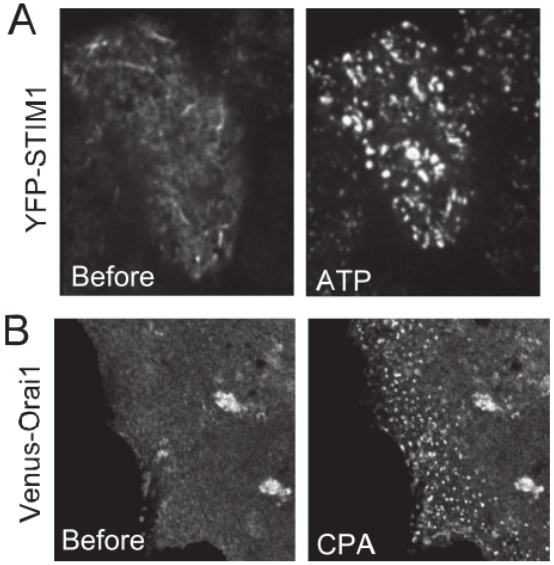

Fig. 2. Rearrangement of STIM1 and Orai1 following store depletion. In panel A, HSY cells expressing YFP-STIM1 were stimulated with ATP in Ca^{2+}-free medium. In panel B, COS-7 cells expressing Venus-Orai1 were stimulated with cyclopiazonic acid (CPA), an ER Ca^{2+} pump inhibitor, in Ca^{2+}-free medium. Modified from Ref. 38 with permission.

YFP-stim1 interacts with plasma-membrane: TIRF

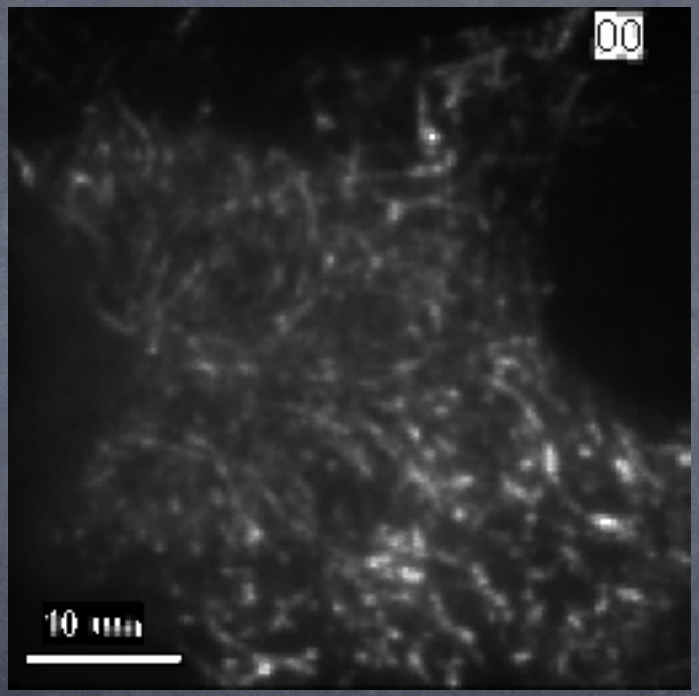

Biochemical and Biophysical Research Communications 460 (2015) 40–49

Contents lists available at ScienceDirect

Biochemical and Biophysical Research Communications

journal homepage: www.elsevier.com/locate/ybbrc

Review

Store-operated calcium entry: Mechanisms and modulation

Patrick G. Hogan*, Anjana Rao

La Jolla Institute for Allergy & Immunology, 9420 Athena Circle, La Jolla, CA 92037, USA

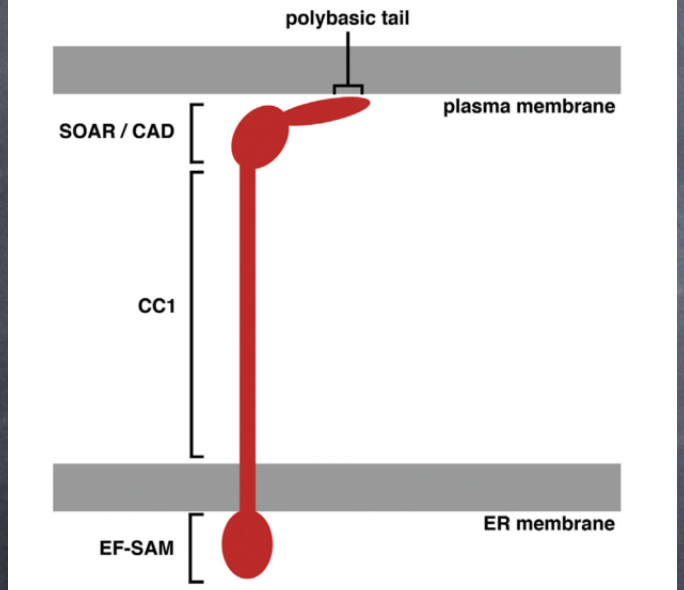

Fig. 1. Cartoon view of STIM1 in an extended conformation, bridging the distance from ER to plasma membrane. For clarity, a single STIM monomer is shown, but the active extended form in cells is oligomeric. Functional regions of STIM discussed in the text are the calcium-sensing EF-SAM domain in the ER lumen, the cytoplasmic CC1 region that both stabilizes inactive STIM and transmits the activating conformational change upon ER calcium store depletion, the SOAR/CAD domain that recruits and gates ORAI channels, and the polybasic tail that interacts with plasma membrane phosphoinositides.

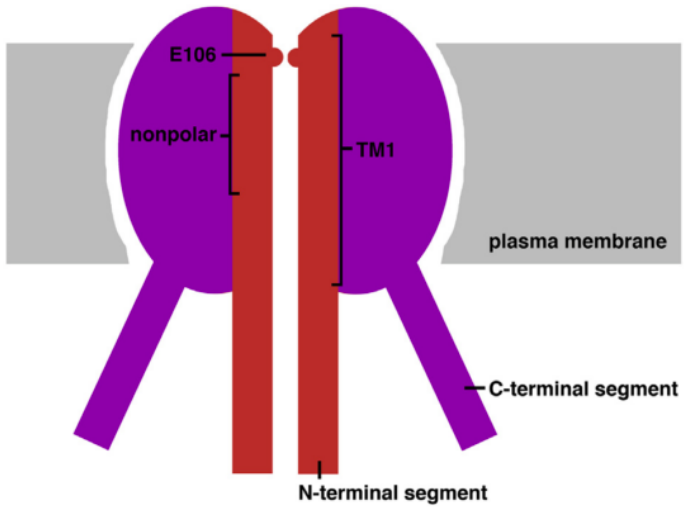

Fig. 2. Cartoon view of the ORAI1 channel. Only two subunits of the hexameric channel are depicted. Labelled are the pore-lining transmembrane helices (TM1), the E106 residues that form a calcium-binding site, the nonpolar region of the pore that constitutes the main barrier to ion flux, and the C- and N-terminal cytoplasmic segments that interact with STIM proteins.

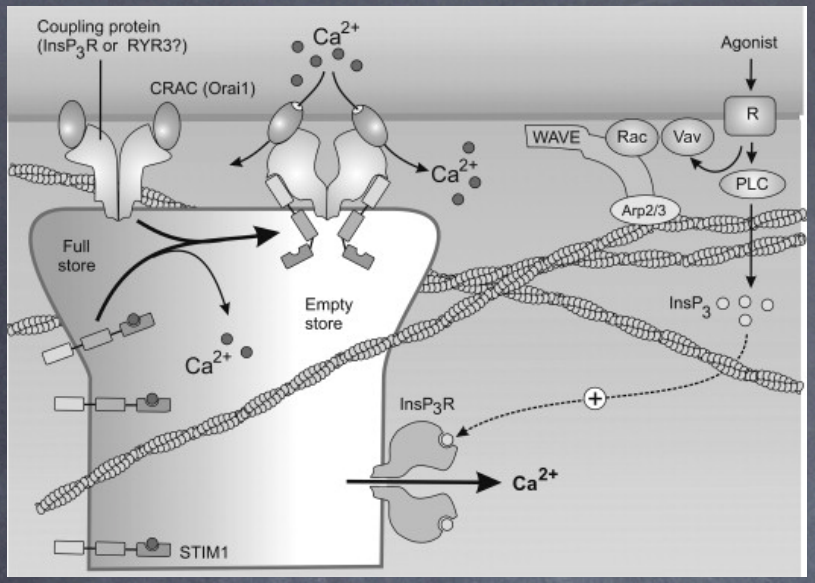

Signalplexes are DYNAMIC

Store-operated calcium entry (SOCE)

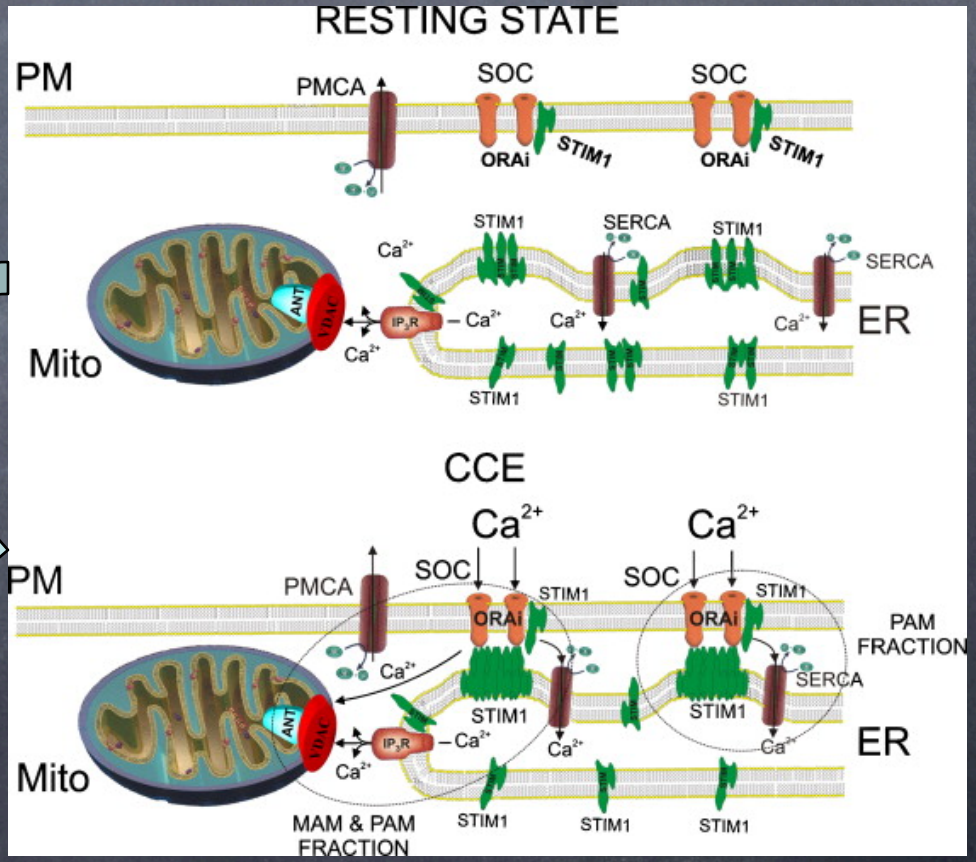

Not only orai1 but also TRP channels…redundancy and variability

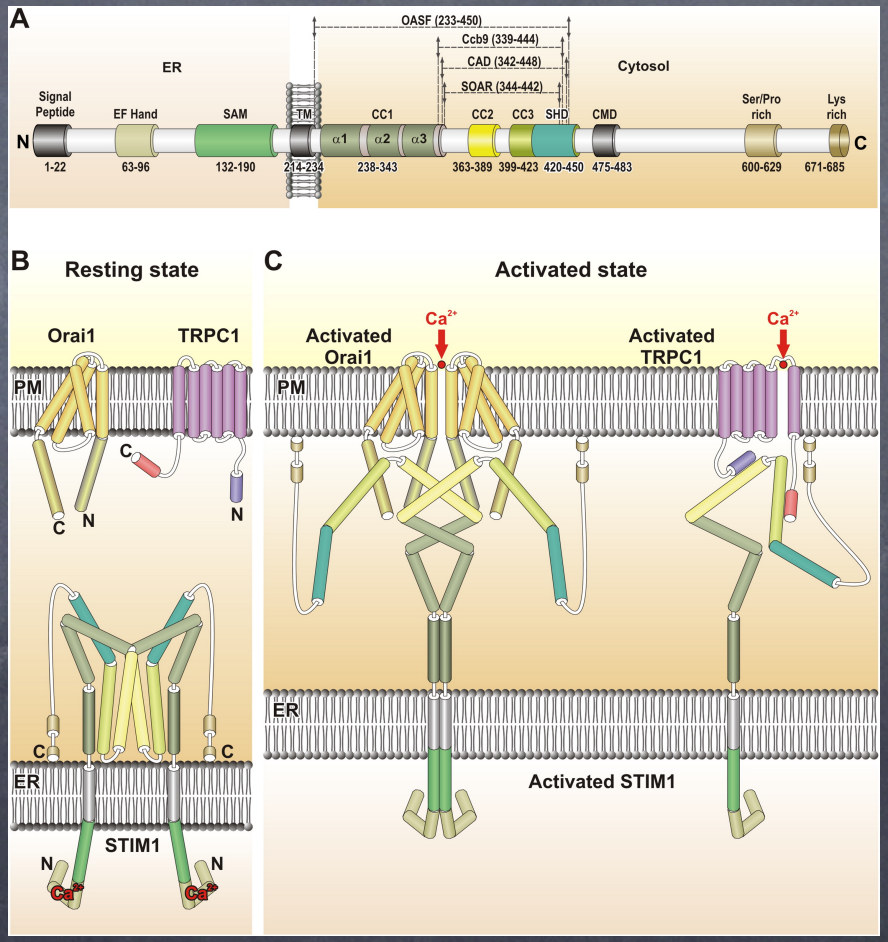

Biochimica et Biophysica Acta 1863 (2016) 2037–2043

Contents lists available at ScienceDirect

Biochimica et Biophysica Acta

journal homepage: www.elsevier.com/locate/bbamcr

Review

Molecular modulators of store-operated calcium entry

Jose J. Lopez [a], Letizia Albarran [a], Luis J. Gómez [a], Tarik Smani [b], Gines M. Salido [a], Juan A. Rosado [a,*]

[a] Department of Physiology (Cell Physiology Research Group), University of Extremadura, 10003 Cáceres, Spain
[b] Department of Medical Physiology and Biophysic, Institute of Biomedicine of Sevilla, Sevilla, Spain

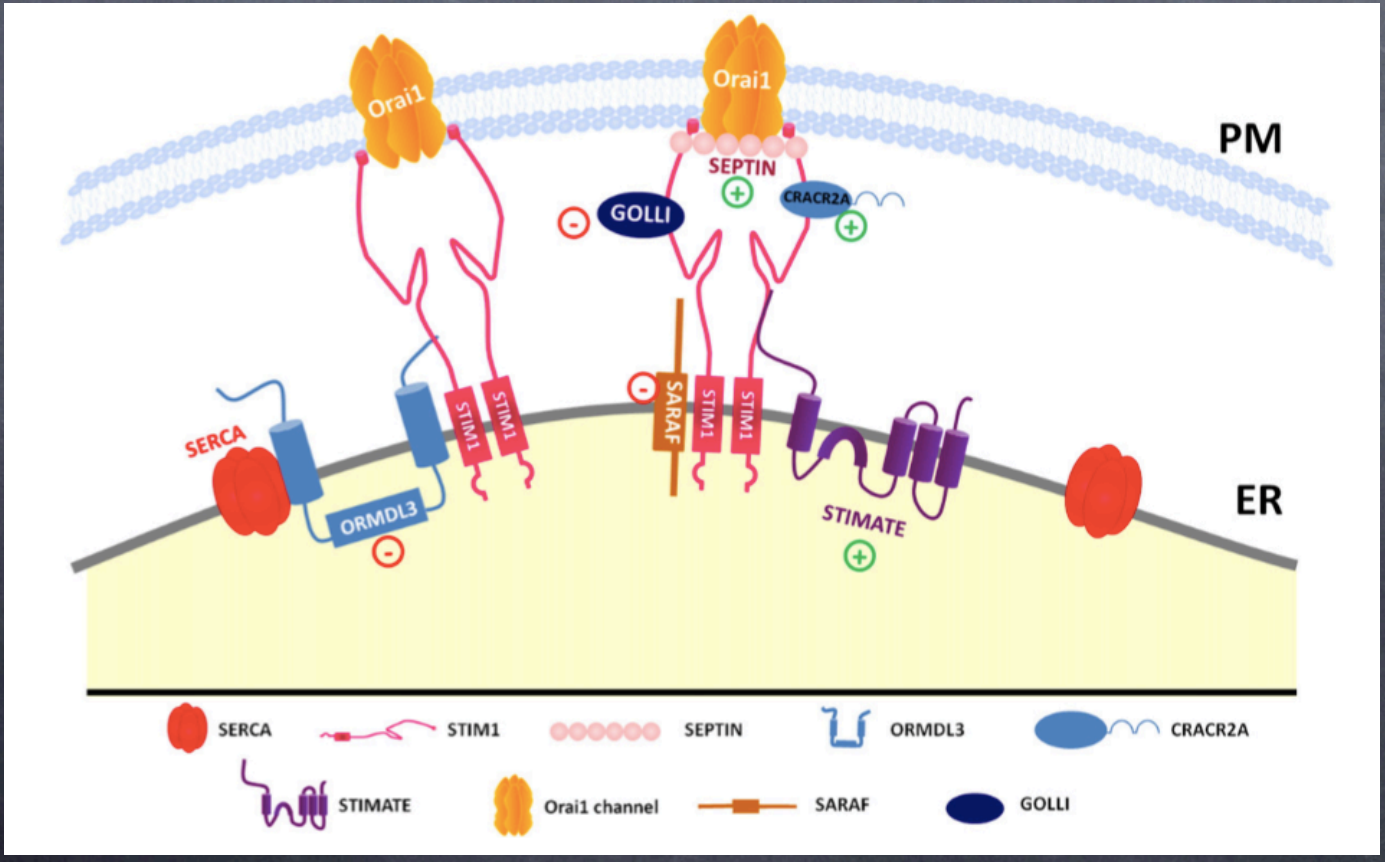

American Physiological Society
Physiological Reviews®

Microdomains of Intracellular Ca^{2+}: Molecular Determinants and Functional Consequences

Rosario Rizzuto, Tullio Pozzan

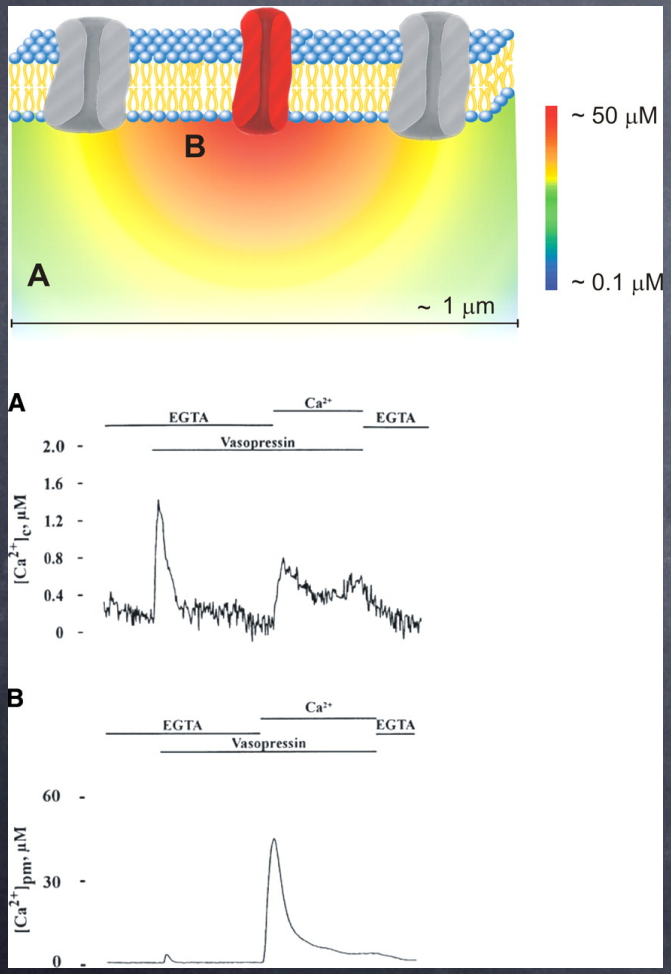

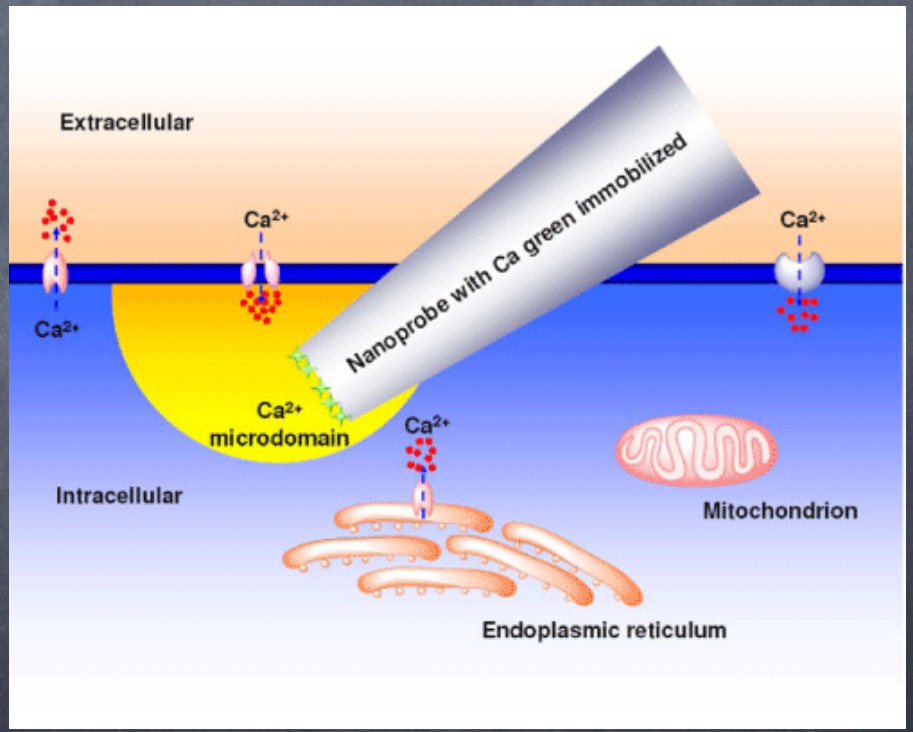

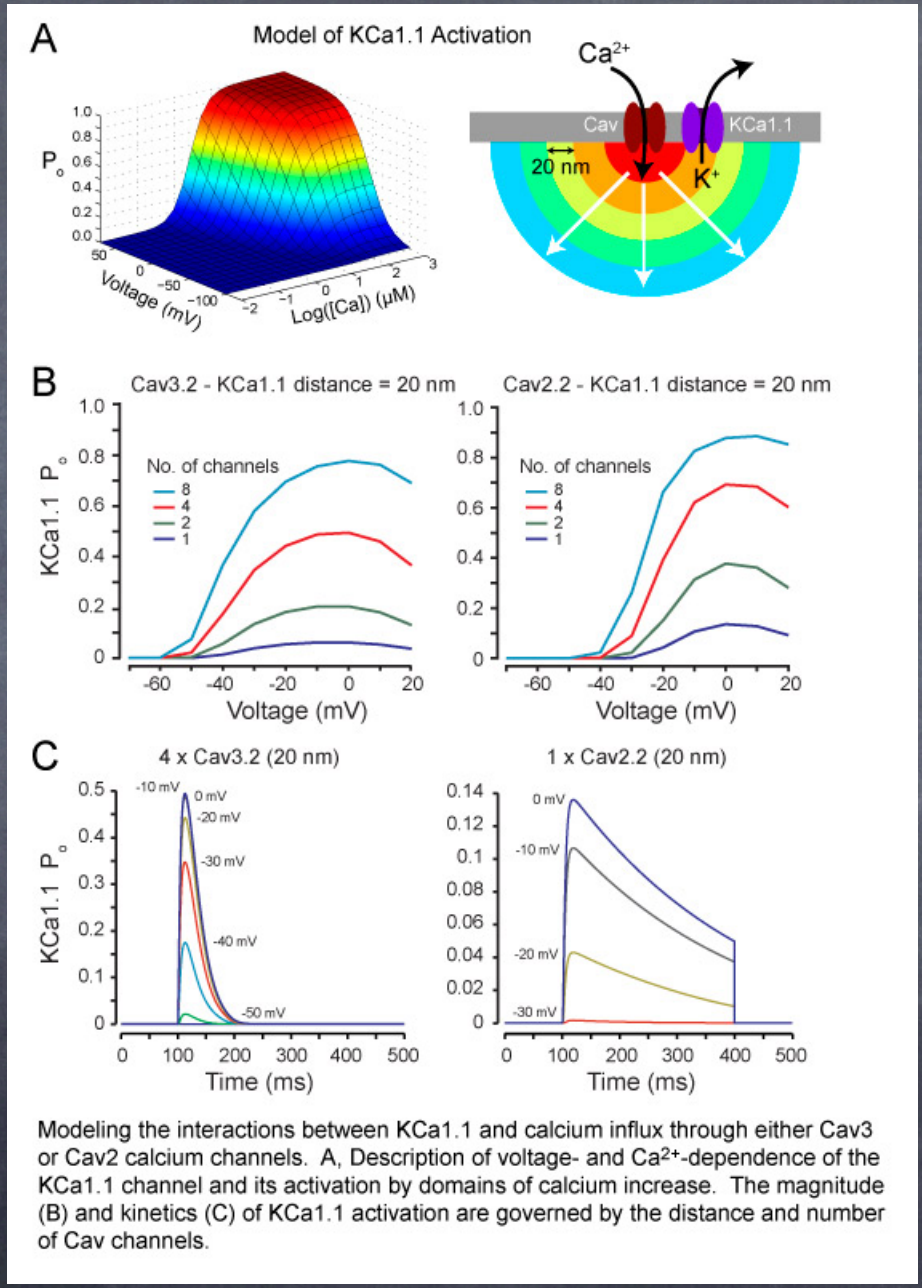

Modeling the interactions between KCa1.1 and calcium influx through either Cav3 or Cav2 calcium channels. A, Description of voltage- and Ca^{2+}-dependence of the KCa1.1 channel and its activation by domains of calcium increase. The magnitude (B) and kinetics (C) of KCa1.1 activation are governed by the distance and number of Cav channels.

HAIR CELLS

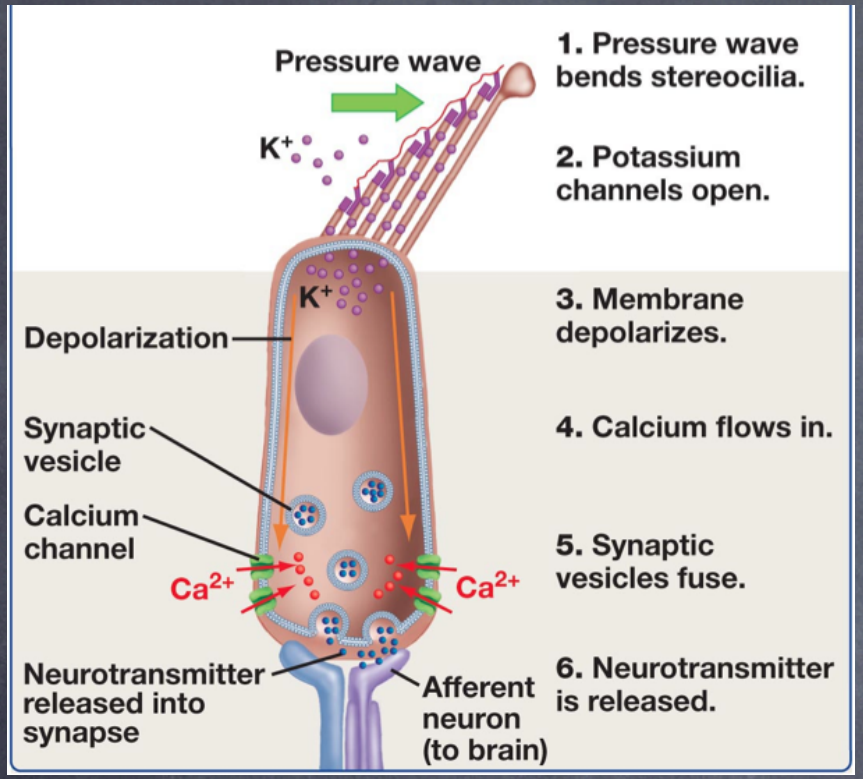
Pressure wave
1. Pressure wave bends stereocilia.
K+
2. Potassium channels open.
K+
3. Membrane depolarizes.
Depolarization
Synaptic vesicle
4. Calcium flows in.
Calcium channel
Ca2+
Ca2+
5. Synaptic vesicles fuse.
Neurotransmitter released into synapse
Afferent neuron (to brain)
6. Neurotransmitter is released.

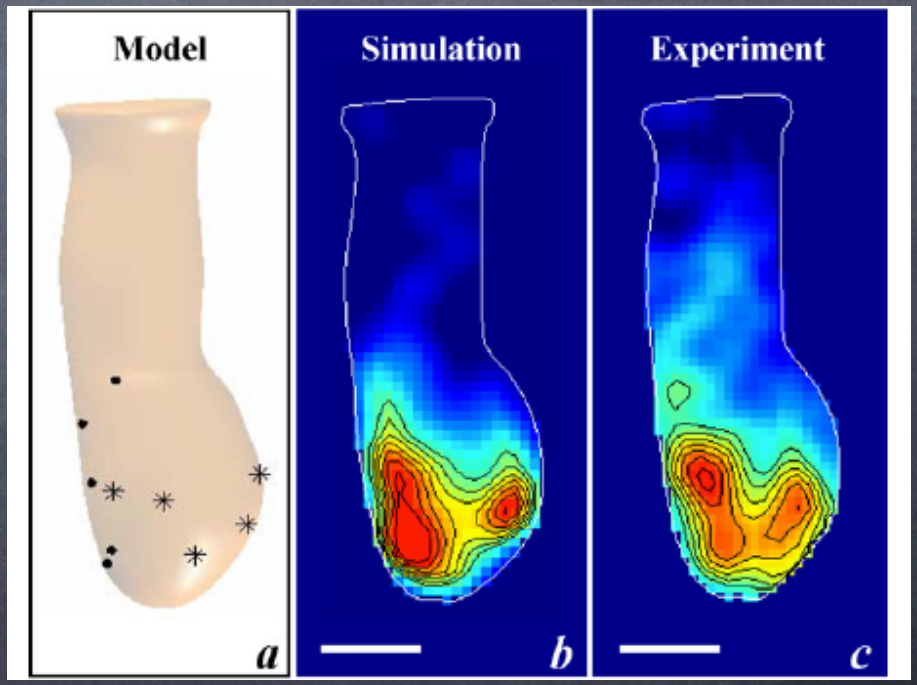
Model
Simulation
Experiment
a
b
c

Polarity in intracellular calcium signaling

Ole H. Petersen,* Denis Burdakov, and Alexei V. Tepikin

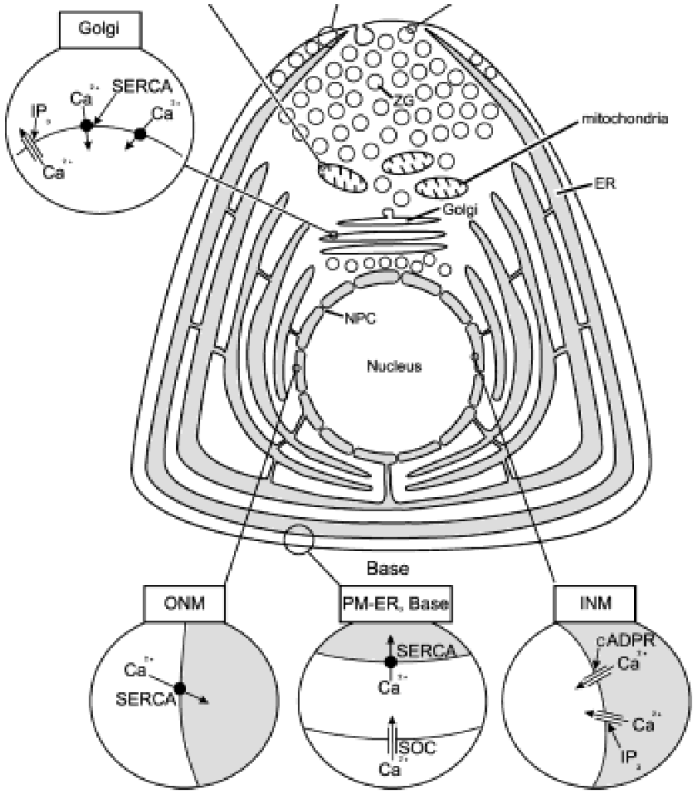

Figure 1. Schematic drawing of a pancreatic acinar cell showing its polarized structure together with the major transport pathways responsible for Ca^{2+} movements in the various parts of the cell. Mito, mitochondria; ER, endoplasmic retieu

Exocytosis, dependent on Ca^{2+} release from Ca^{2+} stores, is regulated by Ca^{2+} microdomains

Jiun T. Low, Alka Shukla, Natasha Behrendorff and Peter Thorn*
School of Biomedical Sciences, University of Queensland, Brisbane, QLD 4072, Australia
*Author for correspondence (p.thorn@uq.edu.au)

calcium

exocytosis

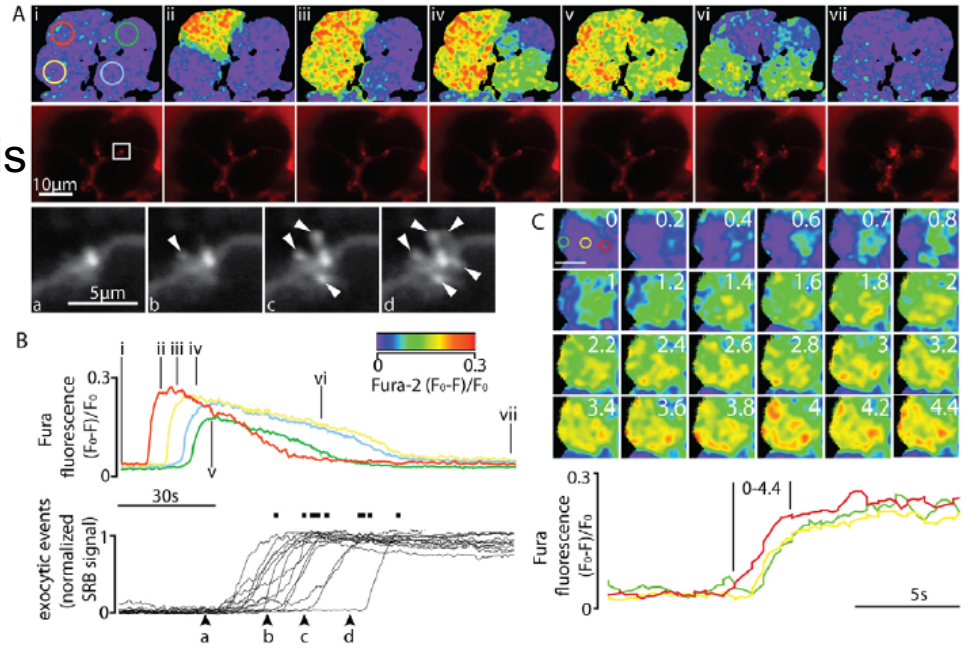

Fig. 1. Ca^{2+} responses within an acinus to CCK stimulation. Cells were loaded with Fura-2 and stimulated by the addition of 20 pM CCK to the bathing solution. (**A**) Within an acinus, individual cells asynchronously show a rise in $[Ca^{2+}]$. (Top and middle rows) Top row: Fura-2 response (F_0-F/F_0 in pseudocolor) at individual time points (i–vii, indicated on the graph in B) throughout the response (blue, low $[Ca^{2+}]$, to red, high $[Ca^{2+}]$). The cell in the upper left responds first, followed sequentially by the other three cells in the group. Middle row: SRB fluorescence (red) that surrounds the cells and diffuses into the lumen between cells. Individual exocytic fusion events, observed as SRB dye enters the granules are seen in the last three images (v–vii). The boxed area in the first image of the middle row indicates the area that is shown enlarged in the four black and white images (a–d). These images show individual exocytic events at time points a–d (arrowheads), indicated on the bottom graph in B. (**B**) Exocytic events follow the Ca^{2+} signals. (Top graph) Average Fura-2 ratiometric response in ROIs within each of the cells (color-coded for each cell, shown in image I in A). (Bottom graph) Time-course of the SRB dye signals in ROIs placed over each individual granule that undergoes fusion (dots above the graph indicate the times of the peaks of each exocytic event). (**C**) Within a single cell, the Ca^{2+} response is seen as a wave spreading from apical to basal regions. The enlarged images show a time sequence of images (0.2 second time intervals) from the lower left-hand cell (shown in A). The Ca^{2+} wave initiates in the apical region (red circle) and then spreads to the basal region (green circle). Scale bar: 10 μm. The graph shows average ratiometric fluorescence changes in each ROI (red, yellow, green) plotted against time. The Ca^{2+} signal rises first in the apical region.

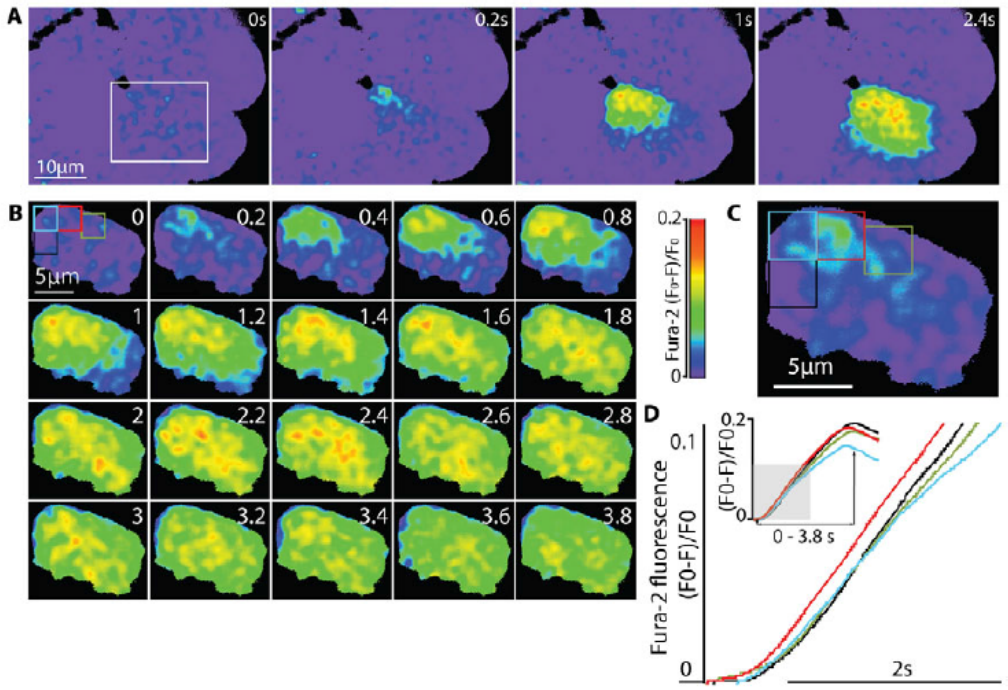

Fig. 5. Identification of the site of origin of the Ca^{2+} wave. Cells stimulated with 20 pM CCK show the Ca^{2+} signal starting at the apical pole and then spreading out across the cell. (**A**) Fura-2 responses (F_0-F/F_0 ratio in pseudocolor) from a CCK-evoked Ca^{2+} response in a single cell within a pancreatic fragment. (**B**) Full sequence of still images from a movie (five frames per second) taken as the Ca^{2+} response spreads across the cell. (**C**) Same cell as in B, enlarged (at the very first movie frame that shows the start of the Ca^{2+} response) with four ROIs of 3×3 µm (boxed areas) centered around the origin of the Ca^{2+} response. (**D**) The main graph is the magnification of the gray-shaded area in inset graph, showing the average fluorescence within each of the ROIs shown in C. The red ROI rises earlier and faster than the surrounding ROIs; for this cell, this region is therefore identified as the point of origin of the Ca^{2+} response.

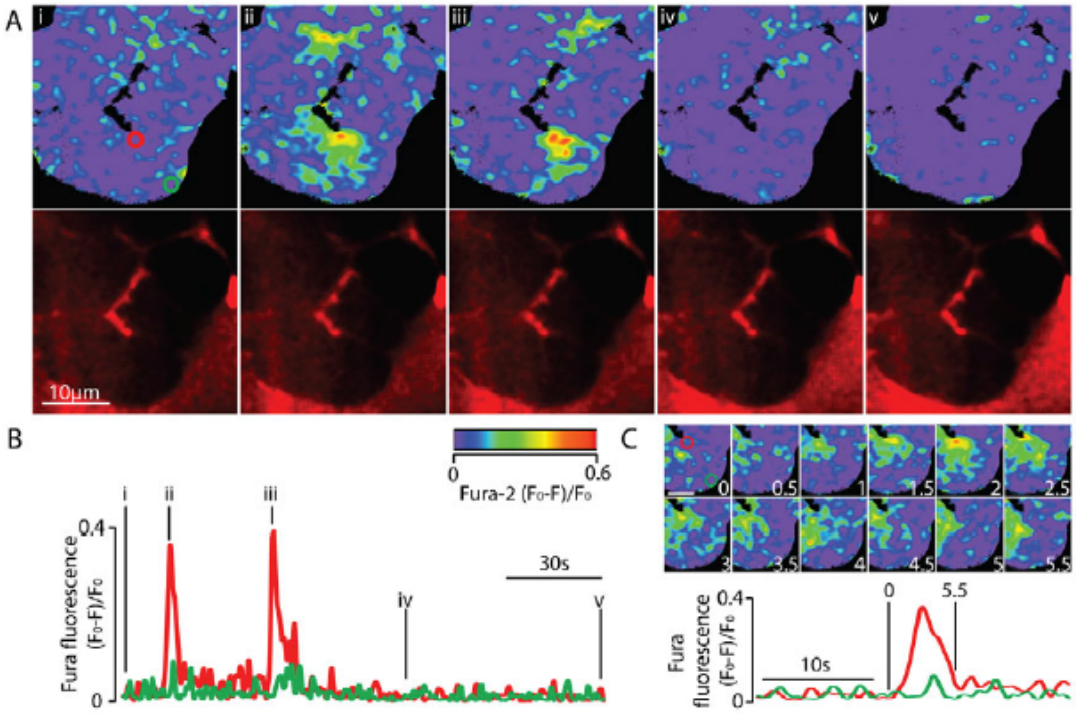

Fig. 9. Local Ca^{2+} spikes do not induce exocytosis. (**A–B**) Upper row of images in A: Fura-2 Ca^{2+} responses (F_0-F/F_0) following stimulation with CCK taken at different time points (i–v; indicated in B). Shown are two consecutive, short-lasting Ca^{2+} spikes that are locally restricted to the apical region (red circle). Lower row of images in A: SRB fluorescence (red). Throughout the occurrence of these local Ca^{2+} spikes there is no change in the SRB signal and no indication of any exocytic events. (B) The large Fura-2 ratiometric changes in the cell from a region of interest placed in the apical pole (red) compared with very little change in a region placed in the basal pole (green). (**C**) The full sequence of images (and the associated graph of average fluorescent changes) taken over the first local Ca^{2+} response clearly shows the spatially restricted nature of the signal.

Invited review

Cell Calcium (1999) **26** (5), 201–208

Article No. ceca.1999.0073

Calcium signal transduction from caveolae

M. Isshiki, R.G.W. Anderson

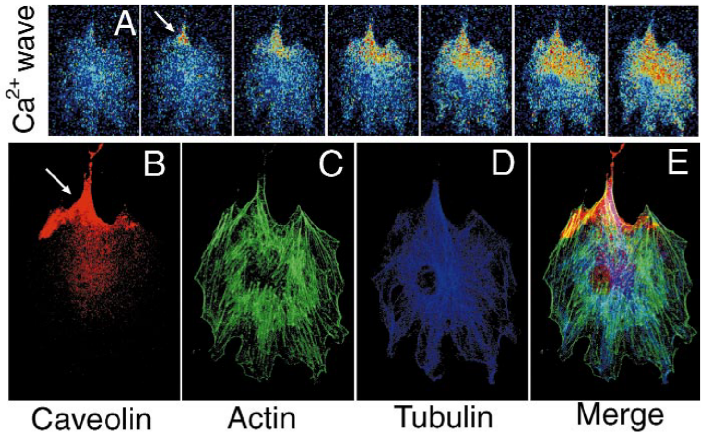

Fig. 1 A Ca^{2+} wave originating at the caveolin-rich cell edge. (A) Sequential images obtained by confocal microscopy showing the origination and propagation of an ATP-induced Ca^{2+} wave at a cell edge of an Indo-1 loaded bovine aortic endothelial cell. Each picture was taken at 0.34 s intervals. (B) The initiation locus of the Ca^{2+} wave in this cell co-localizes with pAb caveolin immunofluorescence (arrow), but seems not to be associated with (C) actin or (D) α-tubulin. A merged image of the three images is shown in E.

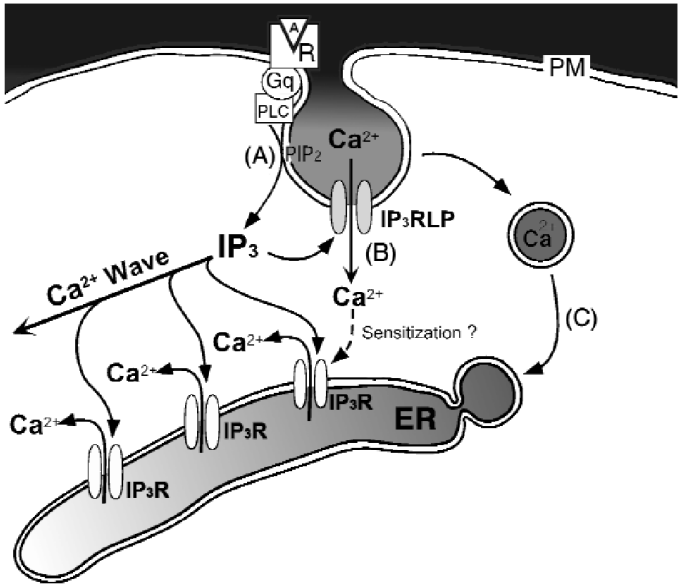

Fig. 2 Three mechanisms (A, B, C) for how caveolae might regulate Ca^{2+} wave initiation. See text for a description.
A: agonist; R: receptor; PLC: phospholipase C; Gq: heterotrimeric $G_{\alpha q}$; PIP_2: phosphatidylinositol 4,5-bisphosphate; IP_3: inositol 1,4,5-trisphosphate; IP_3RLP: IP_3 receptor-like protein; ER: endoplasmic reticulum; PM: plasma membrane.

Electric stimulation of a cardiomyocyte triggers elementary events and then a global calcium wave

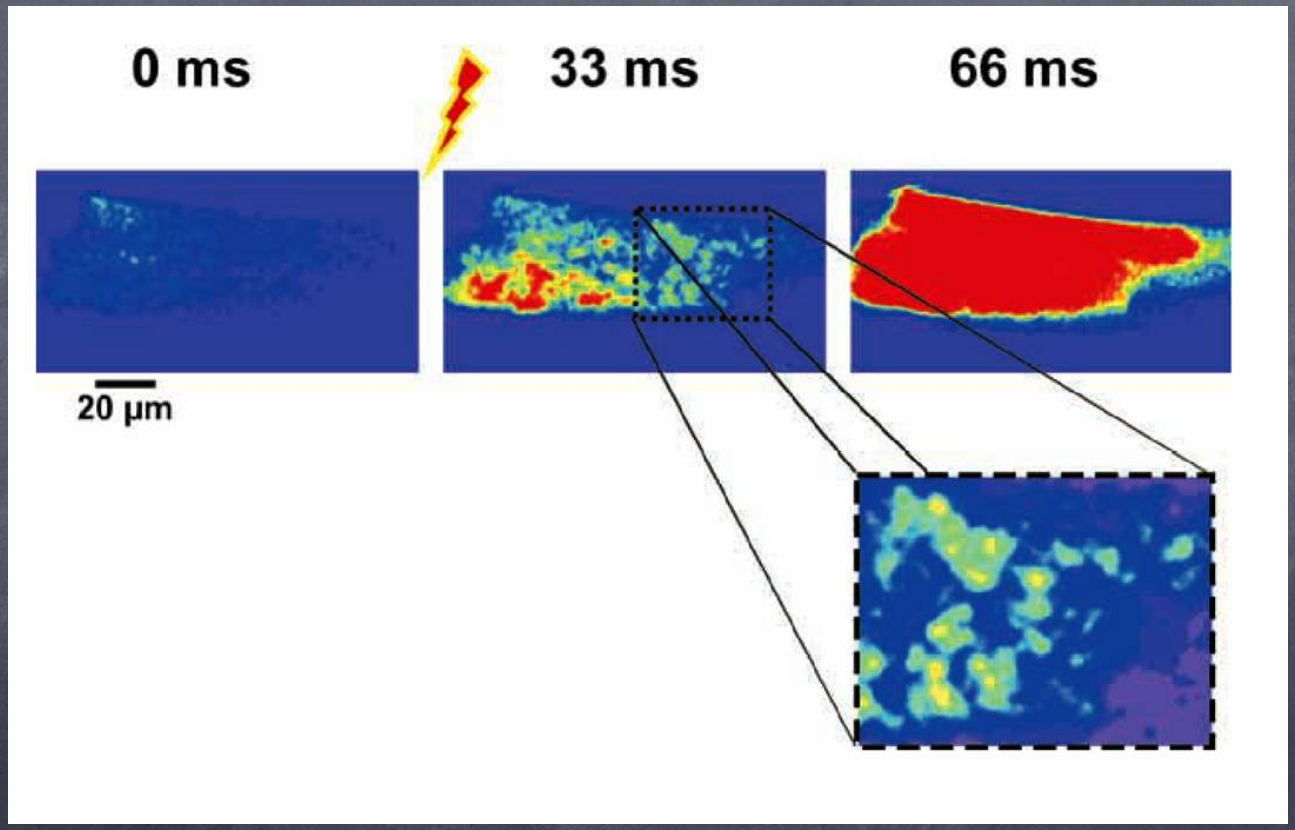

Calcium signalling:

1. perceive spatiotemporal pattern of calcium changes

2. transduce calcium sensors

3. respond calcium effectors and cell response

Calcium-binding domains

EF HANDS: hlh (12-12-12 aa)
loop of 12 aa in which 6 aa are critical for Ca binding
C-term EF hand Kd 10-7 (higher affinity and binds some targets at rest)
N-term Kd 10-6: good sensor

C2-DOMAIN:
PLC (+1 EF-hand motif), PKC, synaptotagmins (Syn)
8-stranded b-sandwich
type I Syn
type II PLC
circular permutation (1 strand of type I is the last in type II)

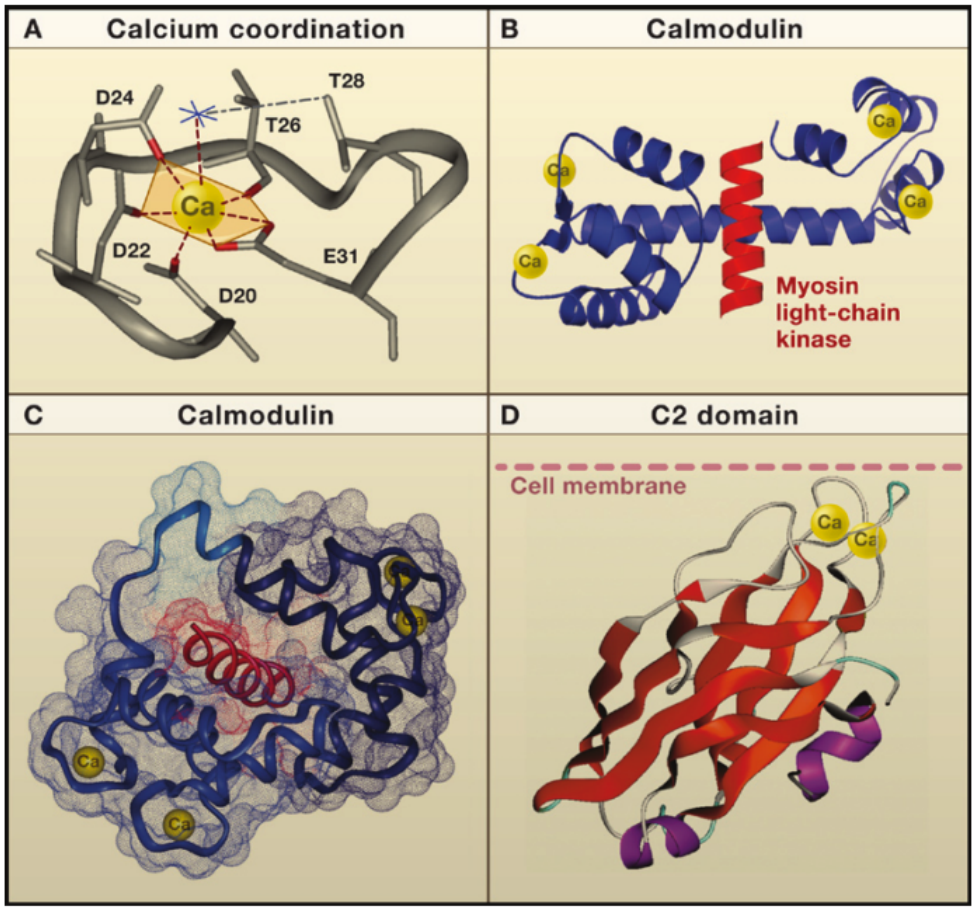

Figure 1. Oxygen Atoms of Amino Acids Chelate Ca^{2+}

(A) Ca^{2+} is coordinated by seven oxygen atoms (five in the plane of the orange pentagon and two perpendicular to the plane, thus forming a bipyramidal pentagon). Adapted from the EF hand calcium-binding proteins data library (http://structbio.vanderbilt.edu/chazin/cabp_database).

(B) Calmodulin has four EF-hand motifs, each with distinct affinities for Ca^{2+}, two at each end of a long jointed α helix. Ca^{2+} binding to calmodulin exposes hydrophobic surfaces. A helical peptide from myosin light chain kinase is colored red. This extended conformation is not stable in solution, but illustrates calmodulin's domains (constructed with Pymol using PDB 3CLN). The red helix represents a hypothetical target peptide.

(C) Ca^{2+}-bound calmodulin wraps around basic amphipathic helices of proteins. Adapted from the EF-Hand Calcium-Binding Proteins Data Library (http://structbio.vanderbilt.edu/cabp_database/cabp.html).

(D) C2 domains bind Ca^{2+} in variable loops containing negatively charged amino acids. The scaffold is an antiparallel β sandwich with an exposed protein-interaction surface. The dashed blue line is the hypothetical plasma membrane (C2 domain of protein kinase C β. PDB 1a25 from the OPM database; http://opm.phar.umich.edu).

CALMODULIN

CaM 148 aa (16 Kd) in all eucaryotic cells
Higher vertebrates: 3 genes highly conserved
4 EF hands
CaMBdomain (higher affinity, nM) of CaMBP: 20aa

CaMBP:
GC, AC, PDE, NOS,
kinases (CaMK (I-V), EFK, IP3K, MLCK),
phosphatases (PP2B or calcineurin)
RNA processing: Smad 1 and 2
Cytoskeleton rearrangement: MAP-2, Tau, spectrin, caldesmon
Plasmamembrane: MARCKS, neuromodulin, neurogranin
PMCA (and via CaMKs SERCA)

Mechanism of activation: inhibition release for CAMKII and calcineurin

Biochemical and Biophysical Research Communications **290,** 615–623 (2002)
doi:10.1006/bbrc.2001.6228, available online at http://www.idealibrary.com on IDEAL®

BREAKTHROUGHS AND VIEWS

Calcium-Binding Proteins: Intracellular Sensors from the Calmodulin Superfamily

Françoise Haeseleer,* Yoshikazu Imanishi,* Izabela Sokal,* Sławomir Filipek,† and Krzysztof Palczewski*,‡,§,[1]

Department of Ophthalmology, ‡Department of Chemistry, and §Department of Pharmacology, University of Washington, Seattle, Washington 98195; and †Department of Chemistry, University of Warsaw, 1 Pasteur Street, PL-02093 Warsaw, Poland

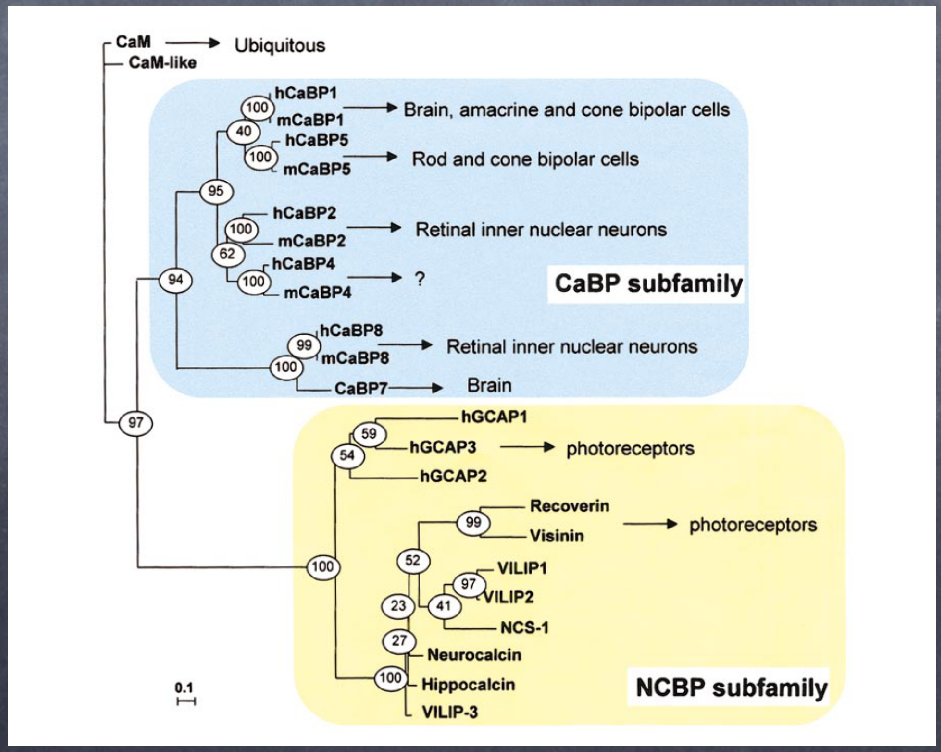

	Nt	EF1	EF2	CENTRAL HELIX	EF3	EF4
		1 12	-2 12		1 12	1 12
hCaM	MADQL	DKDGDGTITTKE	DADGNGTIDFPE	FLTMMARKMKDTDS-----EEEIREAFRVF	DKDGNGYISAAE	DIDGDGQVNYEE
hTropC	MTDQQ	DADGGGDISVKE	DEDGSGTIDFEE	FLVMMV-RQMKEDAK-GKSEEELAECFRIF	DRNADGYIDPGE	DKNNDGRIDFDE
hCaBP1	MGNCV	DKDKDGYINCRD	QINMNLGGHVDFDD	FVELMGPKLLAETAD-MIGVKELRDAFREF	DTNGDGEISTSE	DLNGDGRVDFEE
mCaBP1	MGNCV	DKDKDGYINCRD	QINMNLGGHVDFDD	FVELMGPKLLAETAD-MIGVKELRDAFREF	DTNGDGEISTSE	DLNGDGRVDFEE
hCaBP5	MQFPM	DKDRDGFISCKD	QIRMNLGGRVDFDD	FVELMTPKLLAETAG-MIGVQEMRDAFKEF	DTNGDGEITLVE	DVNGDGTVDFEE
mCaBP5	MQFPM	DKDQDGFISYKD	QIRMNLGGRVDFED	FVELMTPKLLAETAG-MIGVQEMRDAFKEF	DANGDGEITLAE	DINGDGTVDFEE
hCaBP2	MGNCA	DRDQDGYIGCRE	QIS---GGKVDFED	FVELMGPKLLAETAD-MIGVRELRDAFREF	DTNGDGRISVGE	DLNGDGLVDFEE
mCaBP2	MGNCA	DRDRDGYIGYRE	QIS---GGKVDFED	FVELMGPKLLAETAD-MIGVRELRDAFREF	DTNGDGCISVGE	DLNGDGLVDFEE
hCaBP4	MTTEQ	DTDRDGYISHRE	HIKMRMGGRVDFEE	FVELIGPKLREETAH-MLGVRELRIAFREF	DRDRDGRITVAE	DLNGDGTVDFDE
mCaBP4	MATEH	DTDQDGYIGYRE	HVKMRMGGFVDFEE	FVELISPKLREETAH-MLGVRELRIAFREF	DKDRDGRITVAE	DLNGDGTIDFDE
hCaBP8	MPFHH	DRDGNGFISKQE	DMDGDGQVDFDE	TILGPKLVSSEGRDGFLGNTIDSIFWQFQF	DMQR---ITLEEQF	NEEESLNETMAFIISV
mCaBP8	MPFHH	DRDGNGFISKQE	DMDGDGQVDFDE	TILGPKLVSSEGRDGFLGNTIDSIFWQFQF	DMQR---VTLEEQF	NEEESLNETMAFIISV
CaBP7	MPFHP	DRDGNGFISKQE	DMDGDGQVDFEE	TLLGPKLSTSGIPEKFHGTDFDTVFWKCKC	DMQK---LTVDEKC	TEEESHLGTIAFIISV

FIG. 4. Amino acid sequence alignment of Homo sapiens (prefix h) and *Mus musculus* (prefix m) CaBPs. The four potential EF hand motifs (EF1–4) represent high affinity Ca^{2+} binding sites. Nonfunctional EF hands are shaded. Potential N-myristoylation sites in CaBP1 and CaBP2 are printed white on black. Central helix in CaM is known to undergo major conformational changes upon Ca^{2+} coordination. hTropC, human troponin C.

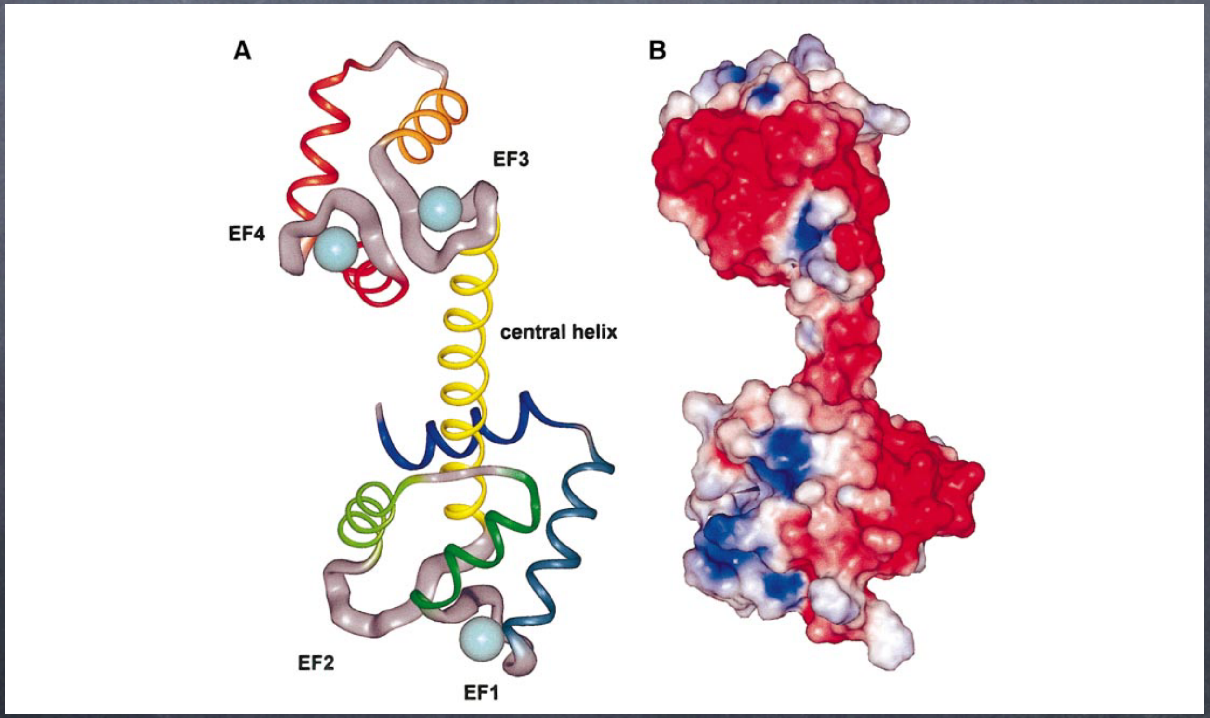

ELSEVIER

Biochimica et Biophysica Acta 1600 (2002) 51–60

BIOCHIMICA ET BIOPHYSICA ACTA
BBA
www.bba-direct.com

Review

Structures, functions and molecular evolution of the penta-EF-hand Ca^{2+}-binding proteins

Masatoshi Maki*, Yasuyuki Kitaura, Hirokazu Satoh, Susumu Ohkouchi, Hideki Shibata

Laboratory of Molecular and Cellular Regulation, Department of Applied Molecular Biosciences, Graduate School of Bioagricultural Sciences, Nagoya University, Furo-cho, Chikusa-ku, Nagoya 464-8601, Japan

Received 15 June 2002; accepted 20 September 2002

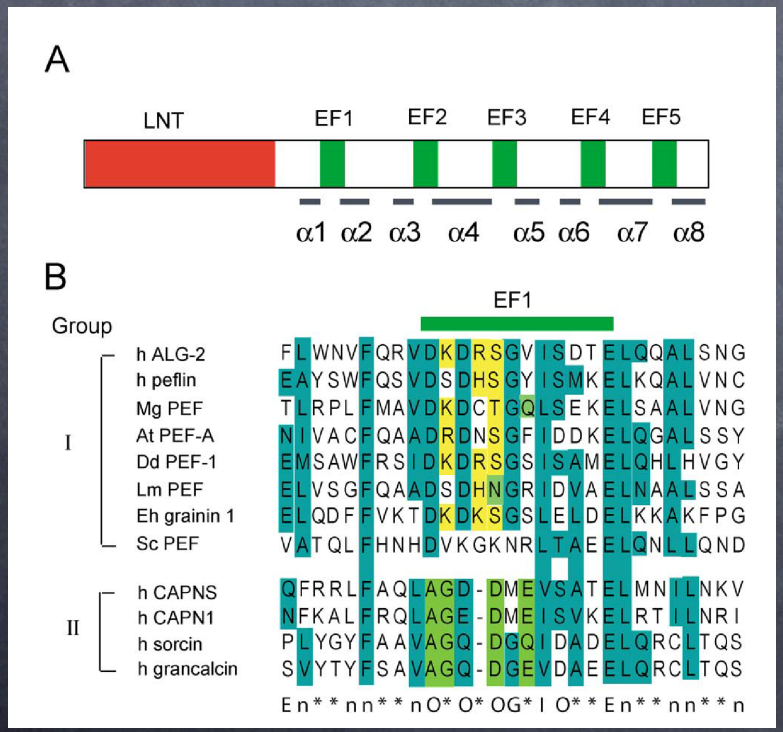

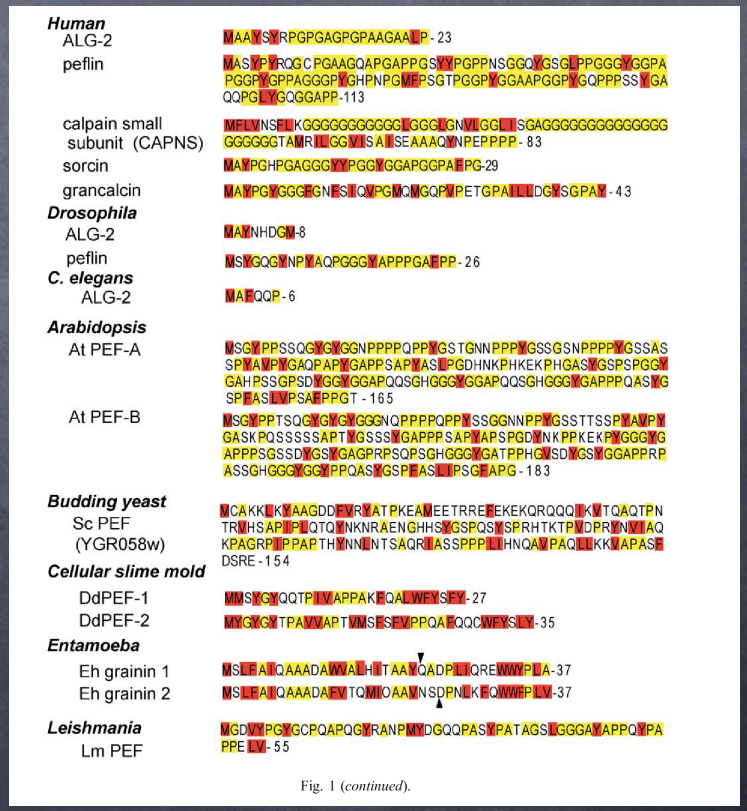

Fig. 1 (*continued*).

Table 1
Presence of PEF protein genes in eukaryotes

PEF genes	Protists	Plants	Fungi	Nematode	Fruit fly	Mammals
Group I						
ALG-2 or analogous proteins	+	+	+	+	+	+
peflin	–	–	–	–	+	+
Group II						
calpain large subunit with PEF domain	–	–	–	–	+	+
small subunit	–	–	–	–	–	+
sorcin	–	–	–	–	–	+
grancalcin	–	–	–	–	–	+

Penta EF hand (PEF) proteins (calpain, peflin, ALG-2, sorcin, grancalcin…) – all eucaryotes
Calpains: cystein proteases
Sorcin: modulation of calcium channels

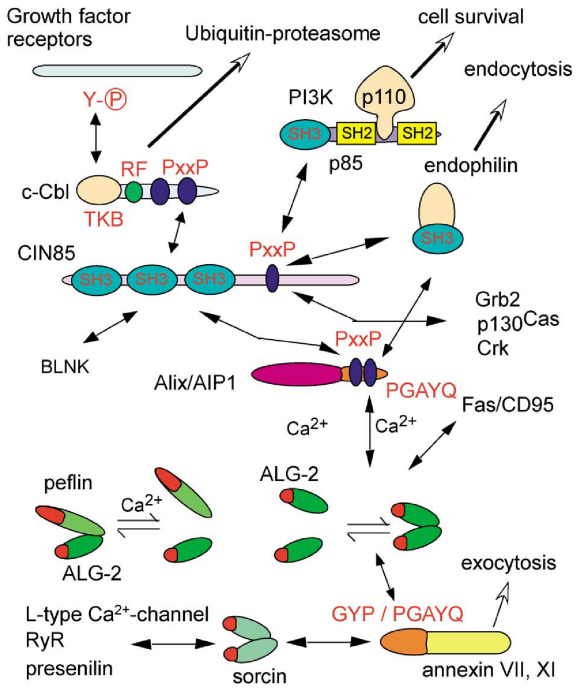

Fig. 3. Interacting protein relationship involving ALG-2. Proteins with known binding regions are shown. PxxP, a core motif for SH3 binding; SH2, Src homology 2; TKB, tyrosine kinase-binding domain; RF, ring finger domain functioning as ubiquitin ligase; Ryr, ryanodine receptor; PGAYQ and GYP, amino acid composition biased regions for potential binding to ALG-2 and sorcin, respectively; BLNK, B cell linker protein [85]. LNT domains of the PEF proteins are colored in red.

doi:10.1016/j.jmb.2003.08.052 *J. Mol. Biol.* (2003) **333**, 621–639

JMB

Available online at www.sciencedirect.com

SCIENCE DIRECT®

ELSEVIER

Functional Recycling of C2 Domains Throughout Evolution: A Comparative Study of Synaptotagmin, Protein Kinase C and Phospholipase C by Sequence, Structural and Modelling Approaches

José L. Jiménez[1,2*], Graham R. Smith[2], Bruno Contreras-Moreira[2] John G. Sgouros[1], Frederic A. Meunier[3], Paul A. Bates[2] and Giampietro Schiavo[4]

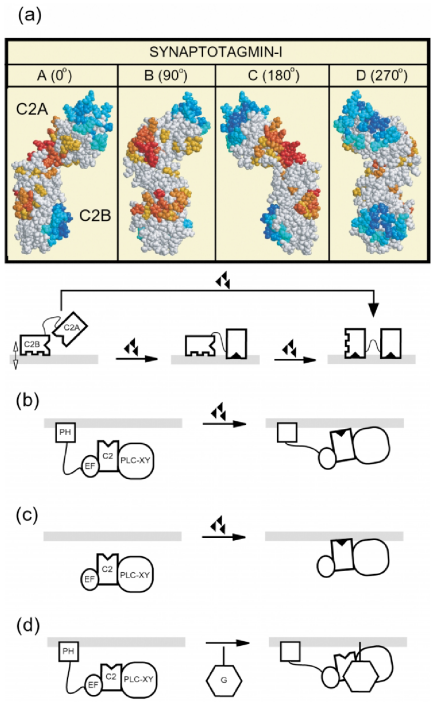

Figure 8. Functional recycling of C2 domains. The Figure shows the functional diversity for C2 domains present in several proteins. (a) An atomic model of Syt I shows the conserved and divergent patches identified by 3D cluster analysis. The different potential steps during Syt action are depicted underneath. The C2 domains are represented as rectangles with a triangular cavity for the calcium-binding site. C2B also presents indentations at one side, which correspond to the lysine-rich region. The membrane is represented as a grey-filled rectangle and the calcium ions as black triangles. The double arrow close to C2B indicates that its binding to the membrane is weak and probably transient. (b–d) Represent models of action for δ, plant and β-PLCs, respectively. The β-PLC model (d) is very simplified and omits the C-terminal region after the C2 domain that is also known to interact with G-proteins on the membrane.

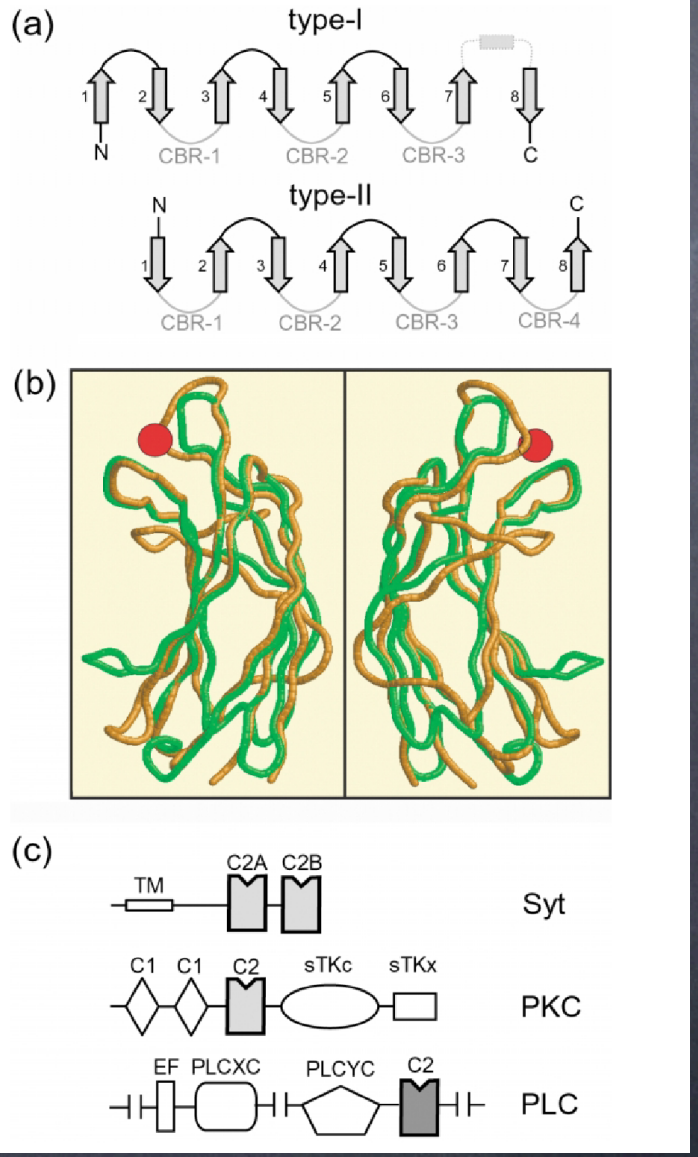

Available online at www.sciencedirect.com
SCIENCE DIRECT®
Genomics 84 (2004) 10–22
GENOMICS
www.elsevier.com/locate/ygeno

Probing the S100 protein family through genomic and functional analysis ☆

Timothy Ravasi,[a,b,*] Kenneth Hsu,[c] Jesse Goyette,[c] Kate Schroder,[a] Zheng Yang,[c] Farid Rahimi,[c] Les P. Miranda,[b,1] Paul F. Alewood,[b] David A. Hume,[a,b] and Carolyn Geczy[c]

[a] *SRC for Functional and Applied Genomics, CRC for Chronic Inflammatory Diseases, University of Queensland, Brisbane 4072, QLD, Australia*
[b] *Institute for Molecular Bioscience, University of Queensland, Brisbane 4072, QLD, Australia*
[c] *Cytokine Research Unit, School of Medical Sciences, University of New South Wales, Sydney 2052, NSW, Australia*

Received 25 November 2003; accepted 2 February 2004

Available online 10 May 2004

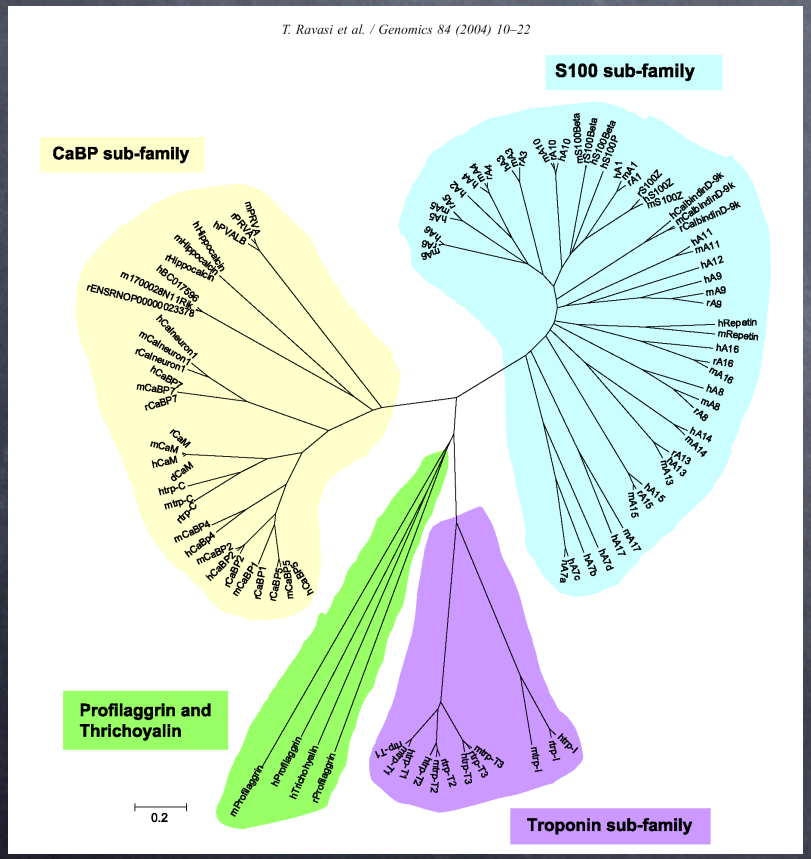

Table 1
Human, mouse, and rat EF-hand superfamily

Proposed gene symbol	Mouse nucleotide accessions No.	Mouse Chr/band	Rat nucleotide accessions No.	Rat Chr/band	Human nucleotide accessions No.	Human Chr/band
S100A1	NM_011309	3f2	S68809	2q34	NM_006271	1q21.3
S100A2	No match[a]	No match	No match	No match	NM_005978	1q21.3
S100A3	NM_011310	3f2	NM_053681	2q34	NM_002960	1q21.3
S100A4	XM_283861	3f2	NM_012618	2q34	NM_019554	1q21.3
S100A5	NM_011312	3f2	AF087469	2q34	NM_002962	1q21.3
S100A6	NM_011313	3f2	NM_053485	2q34	NM_014624	1q21.3
S100A7a	Kulski J.K. et al. 2003	3f2	Kulski J.K. et al. 20003	2q34	XM_048124	1q21.3
S100A7b	Kulski J.K. et al. 2004	3f2	Kulski J.K. et al. 20004	2q34	XM_060509	1q21.3
S100A7c	Kulski J.K. et al. 2005	3f2	Kulski J.K. et al. 20005	2q34	NM_002963	1q21.3
S100A7d	Kulski J.K. et al. 2006	3f2	Kulski J.K. et al. 20006	2q34	XM_060508	1q21.3
S100A7e	Kulski J.K. et al. 2007	3f2	Kulski J.K. et al. 20007	2q34	Kulski J.K. et al. 20003	1q21.3
S100A8	NM_013650	3f2	NM_053822	2q34	NM_002964	1q21.3
S100A9	NM_009114	3f2	NM_053587	2q34	NM_002965	1q21.3
S100A10	NM_009112	3f2	NM_031114	2q34	NM_002966	1q21.3
S100A11	NM_005620	3f2	XM_215598	3q34	MM41341	1q21.3
S100A12	No match	No match	No match	No match	NM_005621	1q21.3
S100A13	NM_009113	3f2	ENSRNOT00000016519	2q34	X99920	1q21.3
S100A14	NM_025393	3f2	RNOR01075109	2q34	NM_020672	1q21.1
S100A15 (2300002L21Rik)[b]	NM_026416	3f2	ENSRNOT00000016499	2q34	NM_080388	1q21.3
S100A17 (5430400H23Rik)[b]	NM_027762	3f2	XM_227375	2q34	XM_060104	1q21.3
S100A16 (A530063N20Rik)[b]	AK041026	3f2	ENSRNOT00000012771	2q34	AL356504	1q21.3
Profilaggrin	AF510860	3f2	AY102923	2q34	M60500	1q21.3
Repetin	NM_009100	3f2	XM_227371	2q34	AL589986	1q21.3
Calneuron1	NM_021371	5f	ENSRNOT00000001184	12q16	NM_031468	7q11.22
Calcium binding protein-1 (CaBP1)	NM_013879	5f	NM_133529	12q16	NM_004276	12q24.31
Troponin T3	NM_011620	7f5	M15202	1q37	NM_006757	11p15.5
Troponin I	NM_009406	7a1	NM_017144	1q12	NM_000363	19q13.42
Troponin T1	NM_011618	7a1	NM_134388	No match	NM_003283	19q13.42
Calcium binding protein-5 (CaBP5)	NM_013877	7a2	ENSRNOT00000020090	1q12	NM_019855	19q13.33
Calcium binding protein-2 (CaBP2)	NM_013878	19a	ENSRNOT00000024770	1q41	NM_031204	11q13.3
Calcium binding protein-4 (CaBP4)	NM_144532	19a	Not available	No match	AC005849	11q13.3
Troponin T2	NM_011619	1f	NM_012676	13q13	NM_000364	1q32.1
Troponin C	NM_009394	2h3	ENSRNOT00000020348	3q42	NM_003279	20q13.12
Hippocalcin	NM_010471	4d2.3	NM_017122	6q14	NM_002143	1p35.1
S100 beta	NM_009115	10b5.3	NM_013191	20p12	NM_006272	21q22.3
Calcium binding protein-7 (CaBP7)	NM_138948	11a1	ENSRNOT00000010439	14q21	ENST00000216144	22q12.2
Calmodulin	NM_007589	12f1	NM_012518	6q31	NM_001743	14q32.11
S100zeta	XM_176783	13d1	ENSRNOT00000024202	2q12	NM_130772	5q13.3
1700028N11Rik[b]	NM_029341	15a2	ENSRNOT00000023378	2q16	BC017596	5p13.2
Parvalbumin-alpha	NM_013645	15e2	NM_002854	22q12.3	NM_022499	7q34
Calbindin D-9k	NM_009789	Xf3	NM_012521	Xq32	NM_004057	Xp22.13
Trichohyalin	XM_195464	3f2	XM_227373	2q34	L09190	1q21
S100P	No match	No match	No match	No match	NM_005980	4p16.1

The genomic location was determined by blasting the corresponding transcripts against the assembly of mouse whole-genome sequence data as described in Materials and methods. Newly described S100 proteins are presented in boldface.
[a] "No match" indicates those genes that we failed to detect in the respective genome.
[b] Newly described members of the EF-hand superfamily.

Review TRENDS in Neurosciences Vol.27 No.4 April 2004

Neuronal Ca^{2+}-sensor proteins: multitalented regulators of neuronal function

Robert D. Burgoyne, Dermott W. O'Callaghan, Burcu Hasdemir, Lee P. Haynes and Alexei V. Tepikin

The Physiological Laboratory, University of Liverpool, Crown Street, Liverpool L69 3BX, UK

Table 1. The NCS and CaBP families of Ca^{2+}-sensor proteins[a]

Protein	Class	Expression in brain or retina	N-terminal myristoylation	Splice variants
NCS proteins				
NCS-1	A	Brain and retina	Yes	None
Hippocalcin	B	Brain	Yes	None
Neurocalcin δ	B	Brain and retina	Yes	None
VILIP-1	B	Brain and retina	Yes	None
VILIP-2	B	Brain	Yes	None
VILIP-3	B	Brain	Yes	None
Recoverin	C	Retina	Yes	None
GCAP1	D	Retina	Yes	None
GCAP2	D	Retina	Yes	None
GCAP3	D	Retina	Yes	None
KChIP1	E	Brain	Yes	1a, 1b
KChIP2	E	Brain	No	2, 2a, 2b
KChIP3	E	Brain	No	?
KChIP4	E	Brain	No	4a, 4b
CaBP proteins				
Caldendrin	CaBP	Brain and retina	Yes and No[b]	Caldendrin, L-CaBP1, S-CaBP1
CaBP2	CaBP	Retina	Yes	L-CaBP2, S-CaBP2
CaBP3	CaBP	Retina	No	None
CaBP4	CaBP	Brain and retina	No	None
CaBP5	CaBP	Retina	No	None

[a]Abbreviations: CaBP, Ca^{2+}-binding protein; GCAP, guanylyl-cyclase-activating protein; KChIP, K^{+}-channel-interacting protein; L-CaBP, long form of Ca^{2+}-binding protein; NCS, neuronal Ca^{2+} sensor; S-CaBP, short form of Ca^{2+}-binding protein; VILIP, visinin-like protein.
[b]L-CaBP1 and S-CaBP1 have N-terminal myristoylation motifs but caldendrin does not.

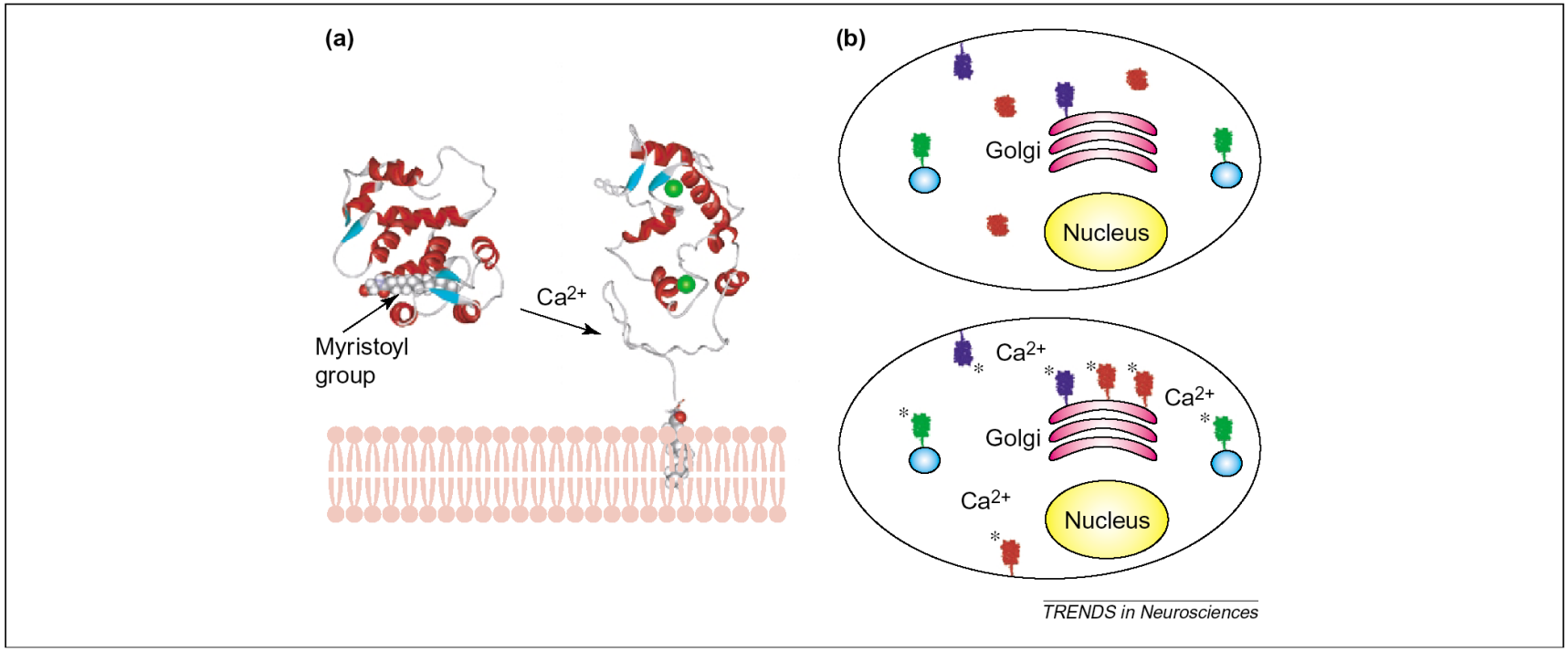

Figure 2. Neuronal Ca^{2+} sensor (NCS) proteins: the Ca^{2+}–myristoyl switch and their intracellular localization. **(a)** The structures of the Ca^{2+}-free (left) and Ca^{2+}-bound (right) forms of recoverin, demonstrating how the binding of two Ca^{2+} ions (green spheres) leads to a conformational change in recoverin [23,24], exposure of the myristoyl group and subsequent membrane association of the protein via the myristoyl group. **(b)** Intracellular distribution of NCS proteins in cells before (top) or after (bottom) Ca^{2+}-level elevation. NCS-1 (dark blue) and K^{+}-channel-interacting protein (KChIP)1 (green) are examples of NCS proteins that are membrane-associated at resting Ca^{2+} concentrations (although they associate with the membranes of different organelles) [29]. Other NCS proteins (red) that possess the Ca^{2+}–myristoyl switch translocate to membrane structures only after elevation of Ca^{2+} concentration [25,27–29]. Active Ca^{2+}-bound forms of the proteins are indicated by asterisks.

multimedia

REVIEW ARTICLE

The neuronal calcium sensor family of Ca^{2+}-binding proteins

Robert D. BURGOYNE[1] and Jamie L. WEISS

The Physiological Laboratory, University of Liverpool, Crown Street, Liverpool L69 3BX, U.K.

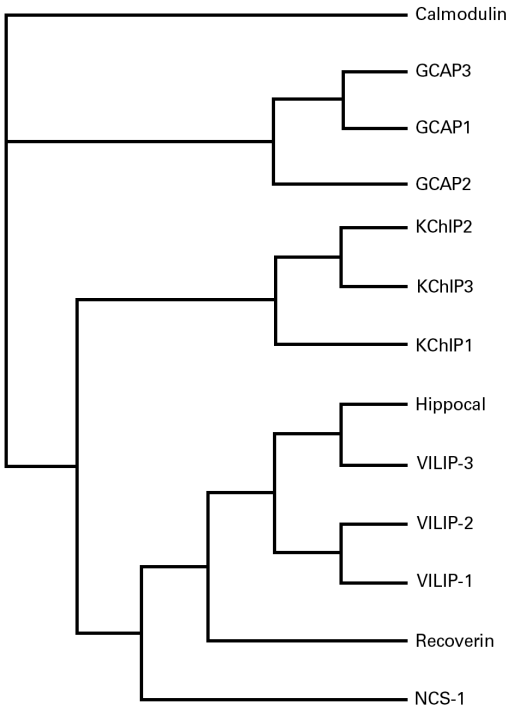

Figure 2 Evolutionary relatedness of the human NCS proteins

A consensus maximum parsimony tree based on the human NCS family members in Figure 1 is shown that was generated using the University of Wisconsin Genetics Computer Group version of the program PAUP [121]. The strict case of 100 maximum parsimony trees is depicted. The consistency index for each of the individual most parsimonious tree used to construct the consensus tree was 0.8.

Calcium signalling:

1. perceive spatiotemporal pattern of calcium changes

2. transduce calcium sensors

3. respond calcium effectors and cell response

Calcium oscillations increase the efficiency and specificity of gene expression

Ricardo E. Dolmetsch*†, Keli Xu* & Richard S. Lewis

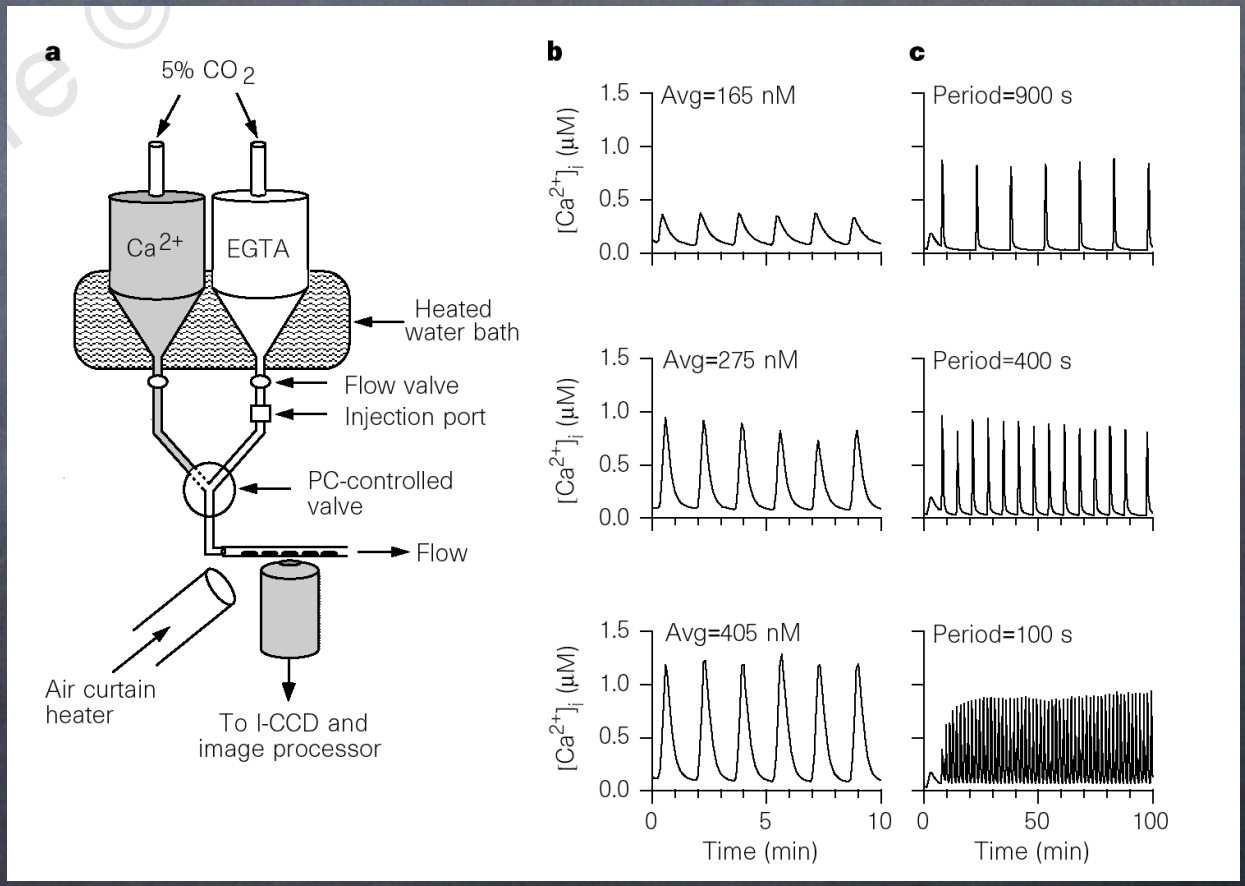

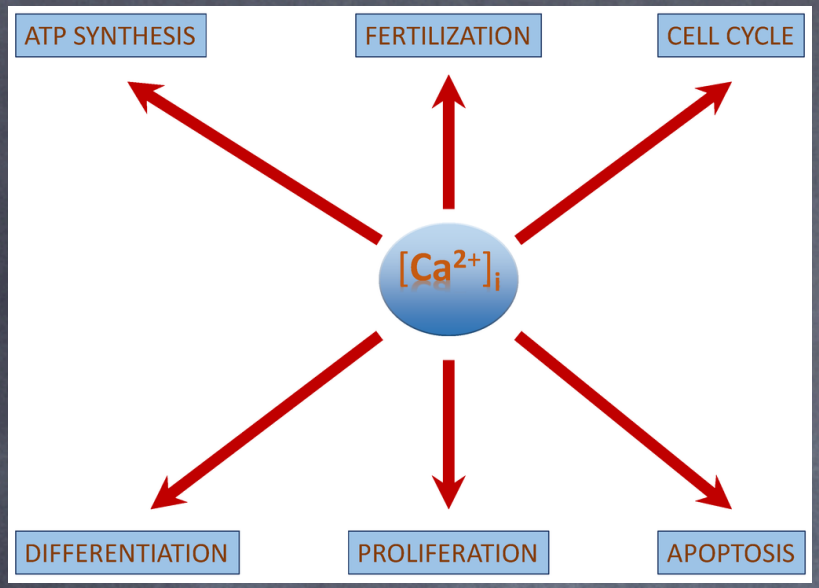
ATP SYNTHESIS
FERTILIZATION
CELL CYCLE
$[Ca^{2+}]_i$
DIFFERENTIATION
PROLIFERATION
APOPTOSIS

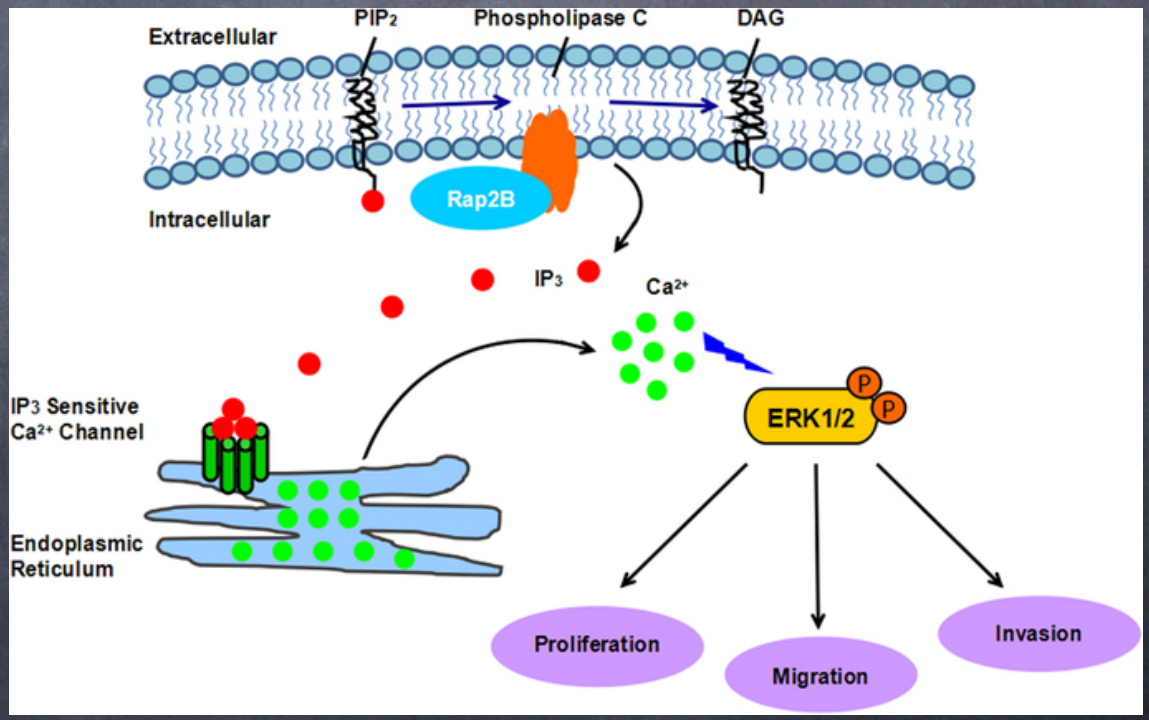
Extracellular
PIP2
Phospholipase C
DAG
Rap2B
Intracellular
IP3
Ca2+
IP3 Sensitive
Ca2+ Channel
Endoplasmic
Reticulum
ERK1/2
P
P
Proliferation
Migration
Invasion

Oocyte fertilization

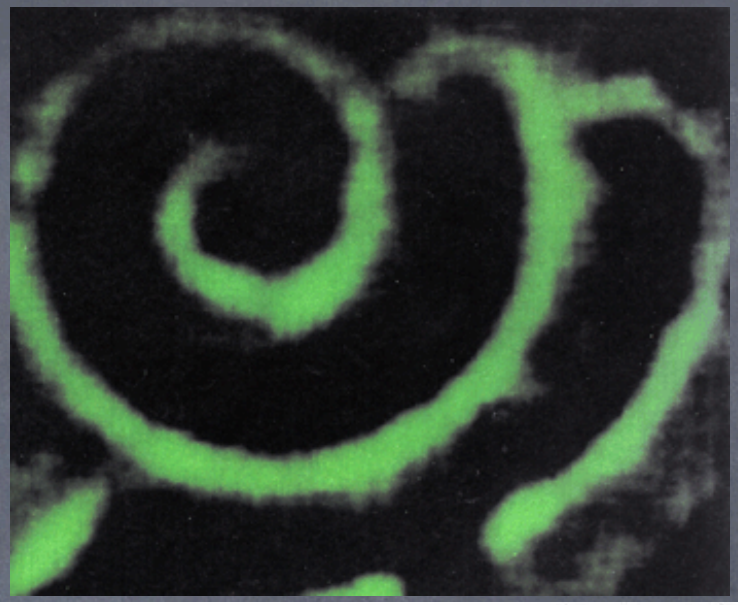

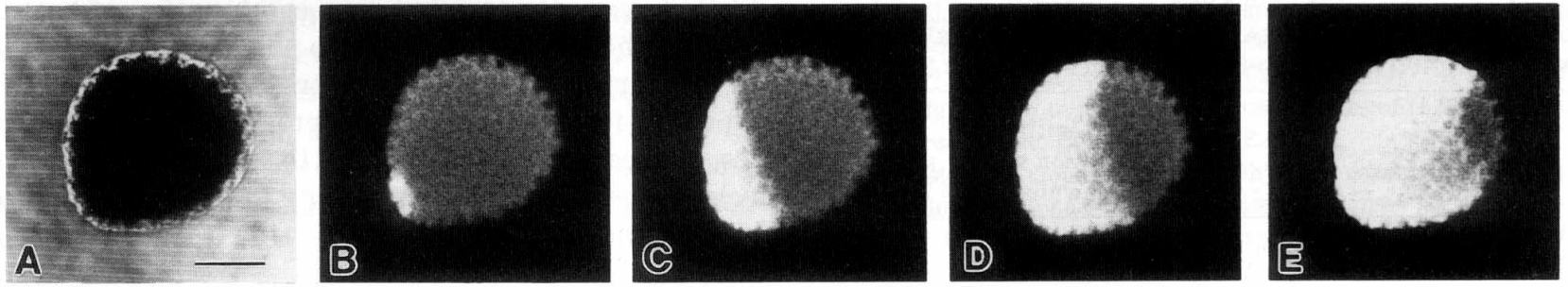

FIG. 6. Wave of fluorescence moving across a Fluo-3-loaded oocyte in MgFSW after the application of $MgCl_2$ solution to the edge of the microinjection chamber. (A) Transmitted light image of the oocyte; bar = 100 μm. (B–E) Confocal microscope images showing the progression of the activation wave; B = 0 time (wave first detected); C = 5 sec; D = 13 sec; E = 23 sec. The oocyte surface is irregular due to the presence of extracellular crypts containing the jelly precursor; jelly release is also a Mg^{2+}-dependent process (Clark *et al.*, 1984).

- From Lindsay et al. (1992). Extracellular Mg^{2+} Induces an Intracellular Ca^{2+} Wave During Oocyte Activation in the Marine Shrimp *Sicyonia ingentis*. Dev. Biol. 152:94-102.

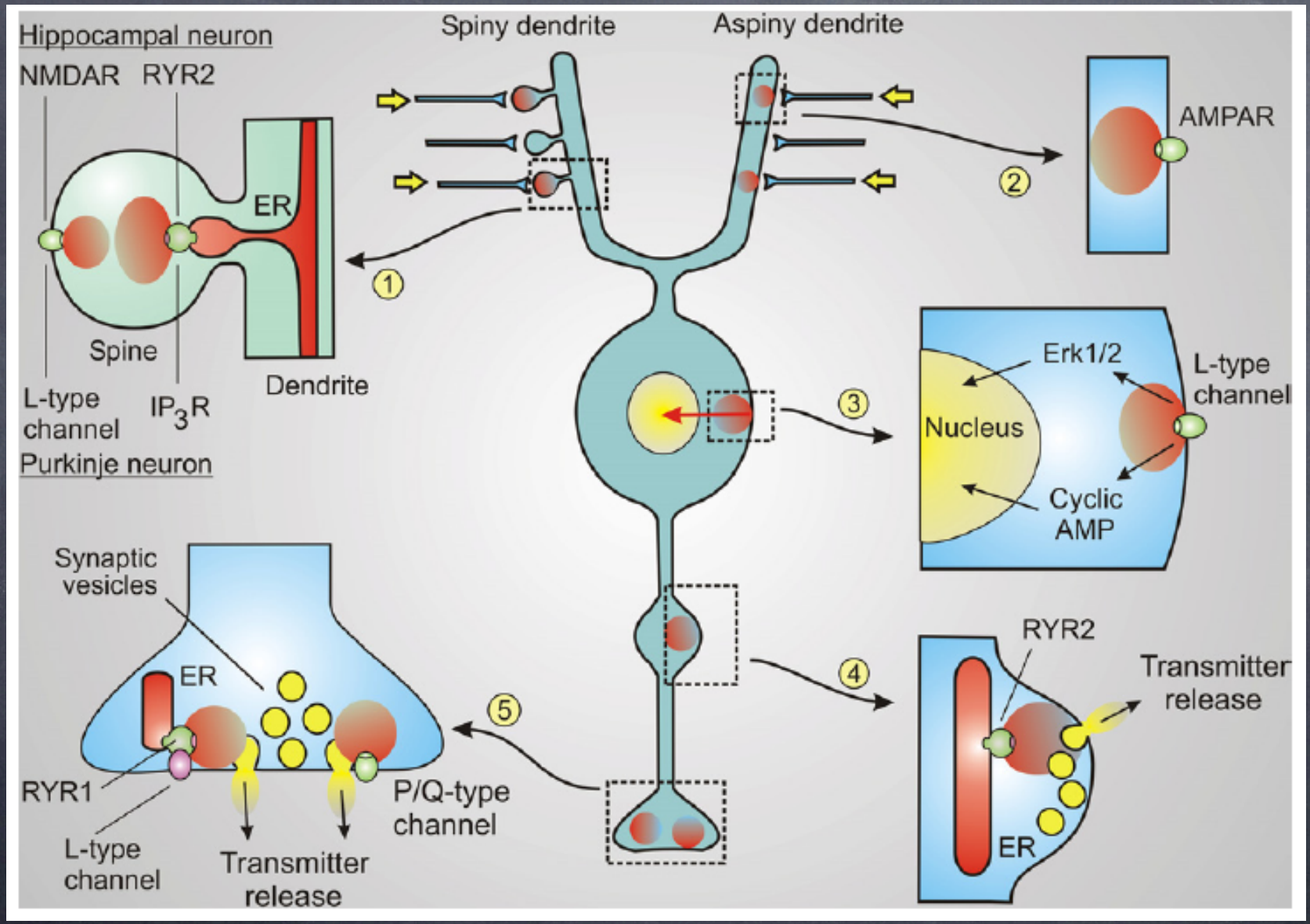
Hippocampal neuron
NMDAR
RYR2
ER
Spine
Dendrite
L-type channel
IP3R
Purkinje neuron
Spiny dendrite
Aspiny dendrite
AMPAR
1
2
3
Erk1/2
L-type channel
Nucleus
Cyclic AMP
4
RYR2
Transmitter release
ER
5
Synaptic vesicles
ER
RYR1
L-type channel
Transmitter release
P/Q-type channel

Polarity in intracellular calcium signaling

Ole H. Petersen,* Denis Burdakov, and Alexei V. Tepikin

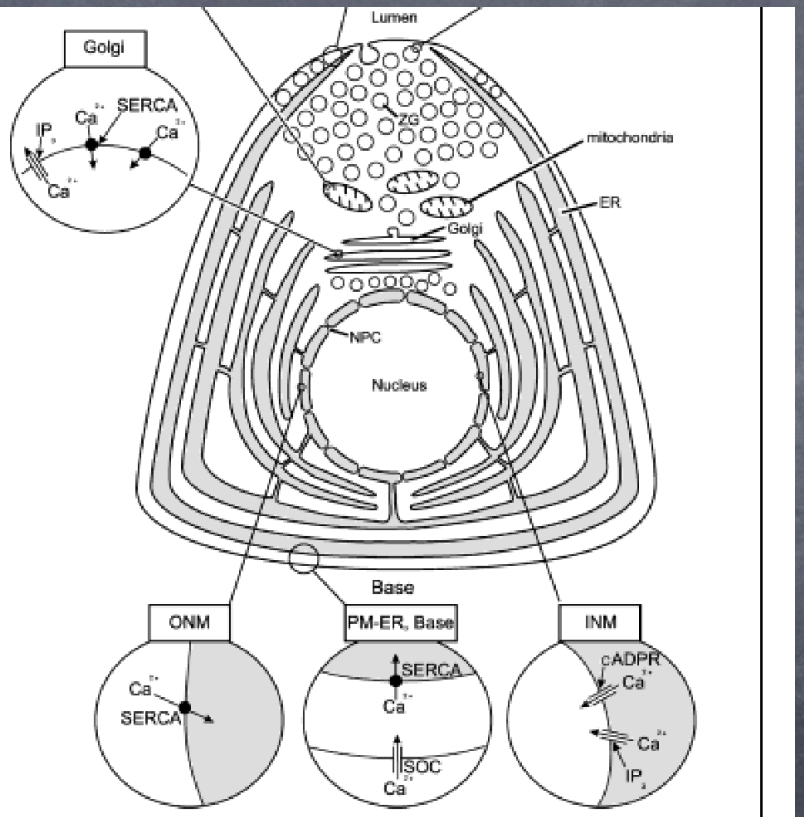

Figure 1. Schematic drawing of a pancreatic acinar cell showing its polarized structure together with the major transport pathways responsible for Ca^{2+} movements in the various parts of the cell. Mito, mitochondria; ER, endoplasmic reticu

Polarization of Calcium Signaling and Fluid Secretion in Salivary Gland Cells

I.S. Ambudkar*

Secretory Physiology Section, Molecular Physiology and Therapeutics Branch, National Institute of Dental and Craniofacial Research, National Institutes of Health, Bethesda, MD 20892

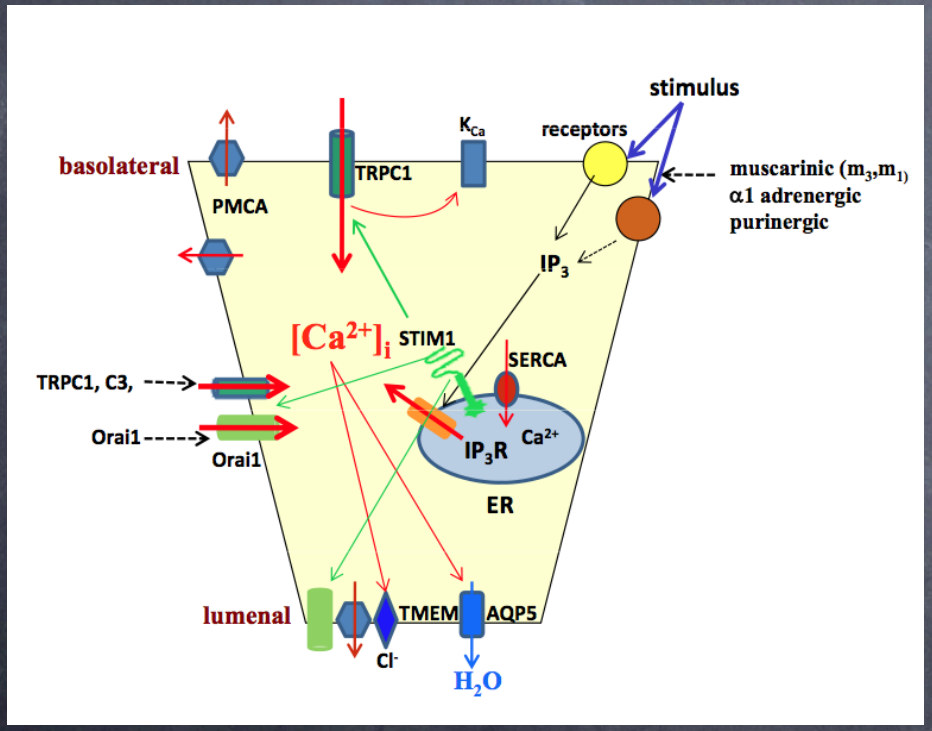

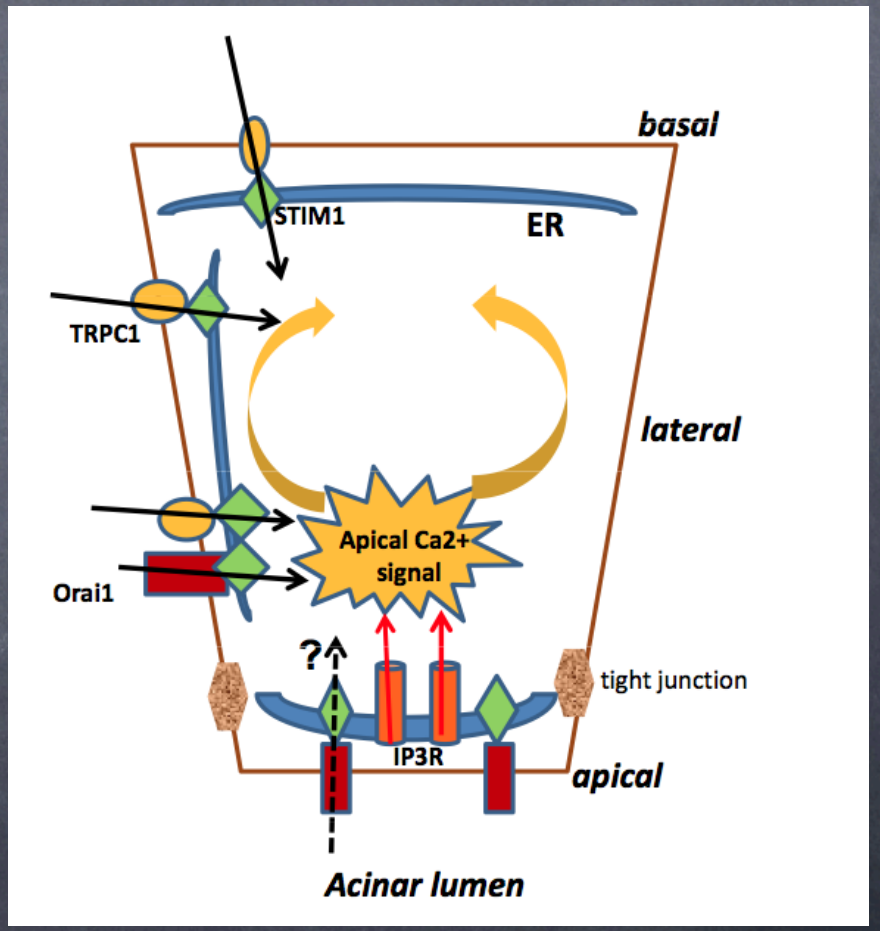

0163-769X/03/$20.00/0
Printed in U.S.A.

Endocrine Reviews 24(6):719–736

doi: 10.1210/er.2003-0008

Regulation of Cell Cycle Progression by Calcium/ Calmodulin-Dependent Pathways

CHRISTINA R. KAHL AND ANTHONY R. MEANS

Department of Pharmacology and Cancer Biology, Duke University Medical Center, Durham, North Carolina 27710

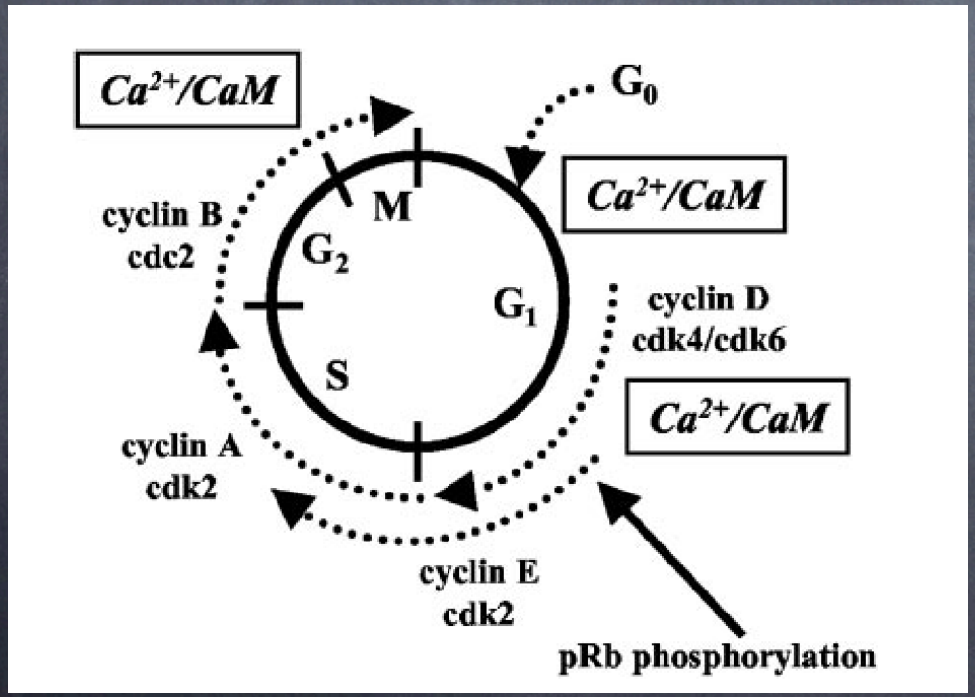

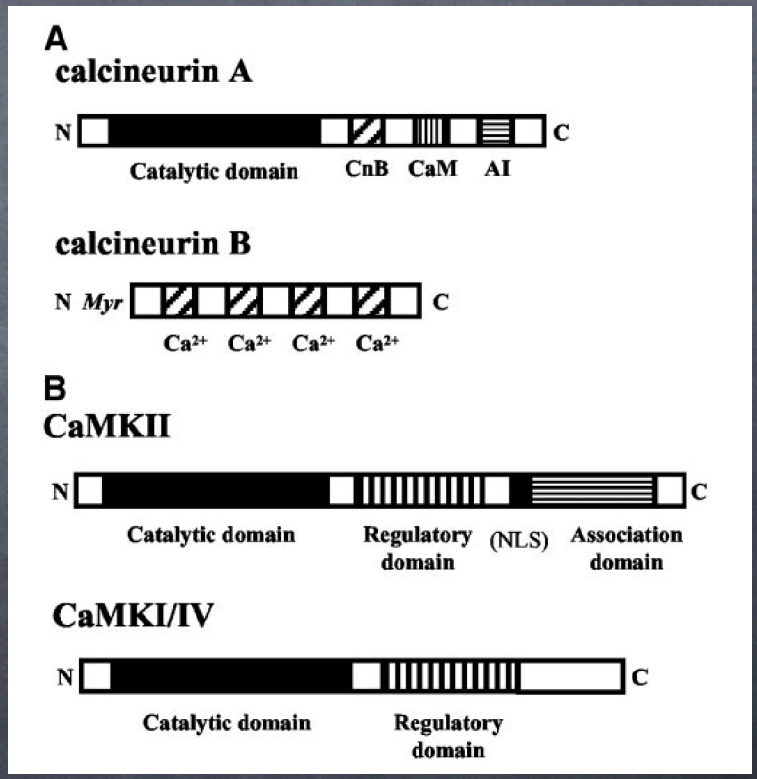

Endothelial cells and angiogenesis: an intriguing model

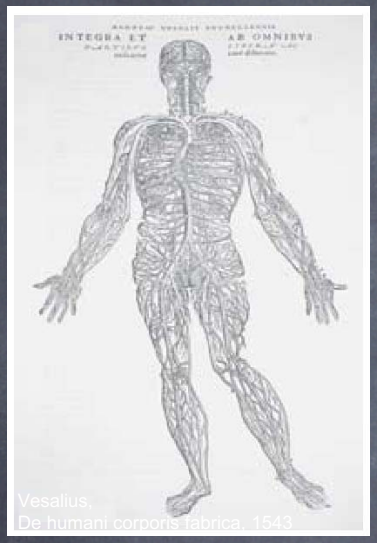
Vesalius,
De humani corporis fabrica, 1543